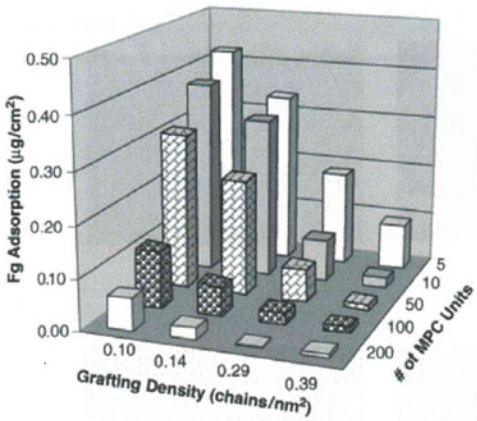

Figure 9. Profile of fibrinogen adsorption on poly(MPC)-grafted silicon surfaces with varying graft density and chain length in a tris-buffered saline buffer for 2 h at room temperature. Fibrinogen concentration: 1.0 mg ml^{-1}. (Reprinted from [91] with permission from Elsevier.)

well-defined graft polymer on a solid surface [83–85]. ATRP has also been applied for the fabrication of polymer brush micropatterns on solid surfaces [62, 86–89]. On well-defined poly(MPC) brushes, protein adsorption was effectively reduced. Furthermore, protein and cell manipulations were easily performed when the thickness of the polymer brushes was just above 5 nm [62, 63, 90]. Preparation of poly(MPC) brushes by ATRP has been reported by Feng and Brash [61, 63, 91]. They prepared PMPC brushes with various graft densities from 0.06 to 0.39 chains nm^{-2} and chain lengths from 5 to 200 MPC units, and characterized their effects on protein adsorption [91]. A marked reduction in fibrinogen adsorption was observed on surfaces with high graft densities and long poly(MPC) chains, as shown in figure 9. These experiments demonstrated the ability of poly(MPC) brushes to considerably reduce protein adsorption and cell adhesion. Yoshimoto and coworkers compared the nonfouling characteristics of a poly(MPC)-modified gold surface and a poly(ethylene glycol) (PEG)-modified gold surface [92]. They clarified that the number of MPC units is an important factor in the excellent protein resistance offered by poly(MPC)-modified gold surfaces fabricated by the 'grafting to' method, which is in sharp contrast to that of PEG-tethered chains.

Polymer brush surfaces have unique friction properties. In particular, the presence of hydrophilic polymer or polyelectrolyte chains is related to the state of water molecules at the interface. The mechanism for high lubrication of poly(MPC) brushes generated on a solid was elaborated by Takahara and co-workers [93, 94]. They prepared poly(MPC) brushes on a silicon wafer via ATRP and characterized the surface properties using a water lubrication system. Poly(MPC) brushes showed an extremely low coefficient of friction even under humid air conditions when probed by a brush-tethered glass ball, probably owing to the adsorption of moisture forming a water-lubrication layer on the surface.

3.2. Biologically specific surfaces based on poly(MPC) brushes

Poly(MPC) brush surfaces can also significantly inhibit lipid vesicle adsorption. Vesicle fusion on patterned PMPC brushes resulted in the preparation of phospholipid bilayer microarrays (PLBMAs), as illustrated in figure 10(a) [80]. A glycolipid containing an oligosaccharide unit for specific binding by cholera toxin B (CTB) subunits was incorporated into phospholipid bilayers containing 2 mol% of ganglioside GM_1. In addition, phospholipid bilayers containing 2 mol% of biotin-cap-DOPE (DOPE stands for 1,2-dioleoyl-sn-glycero-3-phosphoethanolamine) were prepared for specific binding to NeutrAvidin. The binding assay (figure 10(b)) was performed using human plasma as a medium. The fluorescence microscopy images in the left column in figure 10(b) show pure 1,2-dioleoyl-sn-glycero-3-phosphocholine (DOPC) PLBMAs for controls (i and iv). The middle column in figure 10(b) shows PLBMAs with GM_1 (ii and v). The right column shows PLBMAs with biotin-capped lipids (iii and vi). The top row in figure 10(b) shows contact with each PLBMA and the Alexa Fluor 488-labeled 50 nM CTB, whereas the bottom row shows contact with the Alexa Fluor 488-labeled 50 nM NeutrAvidin. As expected, the CTB binds specifically to GM_1-containing PLBMAs (ii). In addition, NeutrAvidin binds specifically to biotin-containing PLBMAs (vi). More importantly, the authors observed neither cross reaction nor non-specific protein binding to lipid bilayer elements that did not contain a ligand other than the one required by the protein–ligand pair of interest (i, iii, iv, v). Similar results were obtained when using phosphate buffered saline instead of human plasma as a medium. These data only demonstrate molecular recognition on PLBMAs using Alexa Fluor 488-labeled proteins. The relevance of PLBMAs as substrates for detection of non-labeled proteins can be clarified using other methods, e.g. enzyme-linked immunosorbent assay.

3.3. Cell-function controllable surfaces

Cell compatibility of MPC polymers has also been determined by measuring the amount of secreted IL-1β mRNA from adherent macrophage-like cells on polymer surfaces [95, 96]. The mRNA expression from the adherent cells on MPC polymer surfaces was significantly lower than that on conventional polymeric biomaterials. This property was the basis for studies of MPC polymers as materials for cell cultivation.

Carbohydrates on a cell surface contribute to most forms of communication between living cells and their environment; therefore, they can also act as surface-immobilized ligands [97]. In particular, galactose residues are preferred conjugated polymers to interact with hepatocytes, which are asialoglycoprotein receptors (ASGPRs). ASGPR is a lectin for receptor-mediated endocytosis found at the hepatocyte cell surface, which is bound to galactose/*N*-acetylgalactosamine (GalNAc)-terminated ligands in a calcium-dependent manner [98, 99]. Although the ASGPR does not function physiologically as an adhesion receptor, galactose-containing

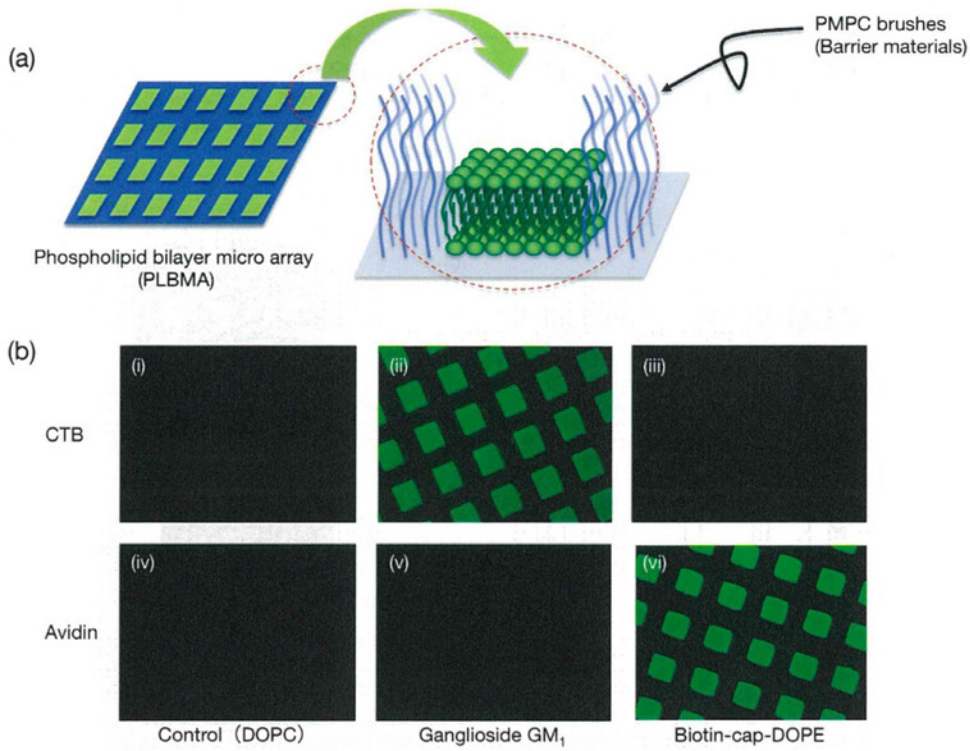

Figure 10. (a) Schematic of phospholipid bilayer microarray (PLBMA) decorated by well-defined poly(MPC) brushes. (b) Fluorescence micrographs of PLBMA containing: (i, iv) DOPC; (ii, v) 2.0 mol% GM_1 in DOPC; (iii, vi) 2.0 mol% biotin-cap-DOPE in DOPC. The top row shows contact with each PLBMA and the Alexa 488-labeled 50 nM CTB (i, ii, iii); the bottom row shows contact with the Alexa 488-labeled 50 nM NeutrAvidin (iv, v, vi) in human plasma.

polymers have been used to induce adhesion in primary hepatocytes [100–102]. Various polymers bearing galactose residues as ligands were prepared for drug delivery [103] and cellular matrices [104]. While these approaches have been quite successful, limitations remain in terms of selective recognition [105]. Indeed, most of the earlier reports did not focus on the reduction of non-specific interactions. Iwasaki *et al* immobilized carbohydrate side chains on PMB37 for inducing specific interactions to cells [106]. They prepared poly(MPC-co-BMA-co-2-lactobionamidoethyl methacrylate) (poly(MPC-co-BMA-co-2-LAMA) or PMBL, figure 11(a)) and coated it on substrates by solvent evaporation. Figure 11(b) shows the density of adherence of the human hepatocellular liver carcinoma cell line (HepG2) having asialoglycoprotein receptors (ASGPRs) and mouse fibroblasts (NIH-3T3) on the polymer surfaces. On poly(BMA), many adherent cells were observed and were well spread with monolayer adhesion, but the cell adhesion was reduced on PMB37. HepG2 adhesion was observed on PMBL. Because the cell has ASGPRs, the number of cells adhering to the PMBL polymer surfaces increased with the density of the galactose residues on the surface. By contrast, adhesion of NIH 3T3 cells to PMBL was reduced in a manner similar to that on PMB because the NIH 3T3 cells did not have ASGPRs. Cell adhesion to the PMBL surface was well regulated by ligand–receptor interactions. Furthermore, some of the cells adhering to the PMBL surface had spheroidal shapes (figure 11(c)), and similar spheroids were scattered on the surface. Although poly(BMA-co-LAMA) (PBL) has galactose residues, the adherent cells were spread as on poly(BMA). The MPC units in PMBL contribute to the spheroidal shape of HepG2 cells. The amount of albumin secreted from a cell was compared with the chemical structure of the substrate. The spheroidal cells cultured on the PMBL surface secreted much more albumin than did the spreading cells that adhered to the poly(BMA). Iwasaki *et al* concluded that the carbohydrate-immobilized MPC polymers produced a suitable interface for biorecognition and preservation of cell functions.

Recent cell engineering has progressed toward regenerative medicine. Soon, cells with superior functions will be obtained and treated by the novel nano- and biotechnologies. Polymeric matrices for cell cultures are very important for achieving these goals. Aliphatic polyesters, such as poly(lactic acid) (PLA), poly(glycolic acid), and their copolymers have been commonly used as matrices for cell cultures [107–109]. These conventional biodegradable polymers are usually highly hydrophobic that hinders penetration of the matrixes by the cell culture medium [110]. Furthermore, significant and non-specific protein adsorption on conventional polymer surfaces makes it difficult to regulate the functions of adherent cells. To overcome these disadvantages of PLA, the MPC polymer is hybridized with PLA by blending [111] and grafting [112]. By controlling the concentration of MPC polymer in the MPC polymer-blended PLA, the inflammatory reaction of adherent cells could be effectively reduced with no decrease in the adherent cell number and proliferation [111].

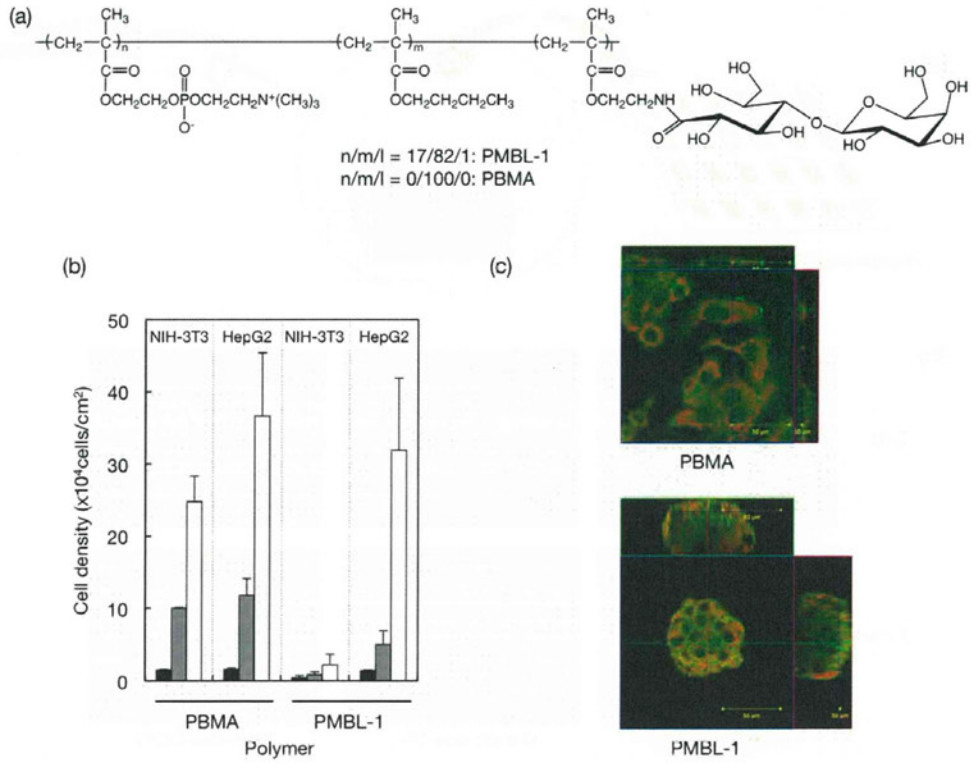

Figure 11. (a) Chemical structure of PMBL. (b) Density of adherent HepG2 and NIH-3T3 on PBMA and PMBL. (c) Confocal micrographs of adherent cells: (green) F-actin and (orange) phospholipid double layer.

Saito *et al* recently proposed an artificial stem cell niche using MPC polymers having a *p*-vinylboronic acid (VPBA) unit (figure 12(a)) [113]. Figure 12(b) shows phase-contrast microscopy images of adhered cells on poly(MPC-co-BMA-co-VPBA) (PMBV352; MPC : BMA : VPBA = 30 : 50 : 20 mol%), PMB37, and conventional tissue culture polystyrene (TCPS). PMB37 without the VPBA unit completely inhibited non-specific cell adhesion. On the other hand, PMBV352, having the VPBA unit, effectively induced cell adhesion despite the surface was fully covered by bioinert phosphorylcholine groups. This result indicated that the VPBA unit induced specific cell adhesion without non-specific protein interactions.

Mesenchymal stem cells, C3H10T1/2, on PMBV352 were differentiated to chondrocyte cells in the presence of a stimulation factor, BMP-2. The real-time polymerase chain reaction (RT-PCR) results are shown in figure 12(c). A chondrocyte marker, Col2a1, was highly expressed from the adhered cells onto PMBV352 with BMP2 signal rather than conventional materials. This result indicates that PMBV352 is a useful artificial stem cell niche to guide the desired differentiation property [114–116].

To extend PMBV from 2D to 3D cell cultivation, water-soluble PMBV was synthesized and mixed with poly(vinyl alcohol) (PVA) for preparing hydrogel matrices. Polymer gelation occurs spontaneously and rapidly when mixing these polymer solutions. This process can be used to encapsulate cells and proteins, and the cell activity can be maintained for more than 7 days [114]. The reaction between boronic acid and multivalent alcoholic compounds was used as the crosslinking mechanism between MPC polymers in an aqueous medium. In a tetrahedral anionic structure, boronic acid produces stable complexes with alcohol compounds including PVA, glucose, etc [117–119]. The hydrogel is reversibly dissociated by the addition of low-molecular-weight compounds such as D-glucose. A new cell maintenance system called a 'cell-container' based on this hydrogel was proposed. By coupling the gelation system and microfluidic technique, encapsulation of a single cell into microgel beads was achieved by Aikawa *et al* [120].

4. Medical devices modified with MPC polymers

4.1. Cardiovascular devices

Figure 13 outlines current applications of MPC polymers in biomedical and other fields. MPC is biocompatible due to the similarities with cell walls. Its polymerizable unit is an ideal new material for contact lenses, eye care products such as contact lens cleanser, cosmetics, toiletries, and medical devices. This biocompatibility will enable the creation of a wide range of applications as discussed in previous review articles [121–123].

As mentioned above, it has been widely shown that surface modifications with MPC polymers are effective in improving blood compatibility by suppressing protein adsorption, platelet adhesion, and platelet activation at blood-contacting surfaces. MPC polymers have recently been applied to improve blood compatibility of blood-contacting and cardiovascular devices such as medical membranes for oxygenators and hemodialysis

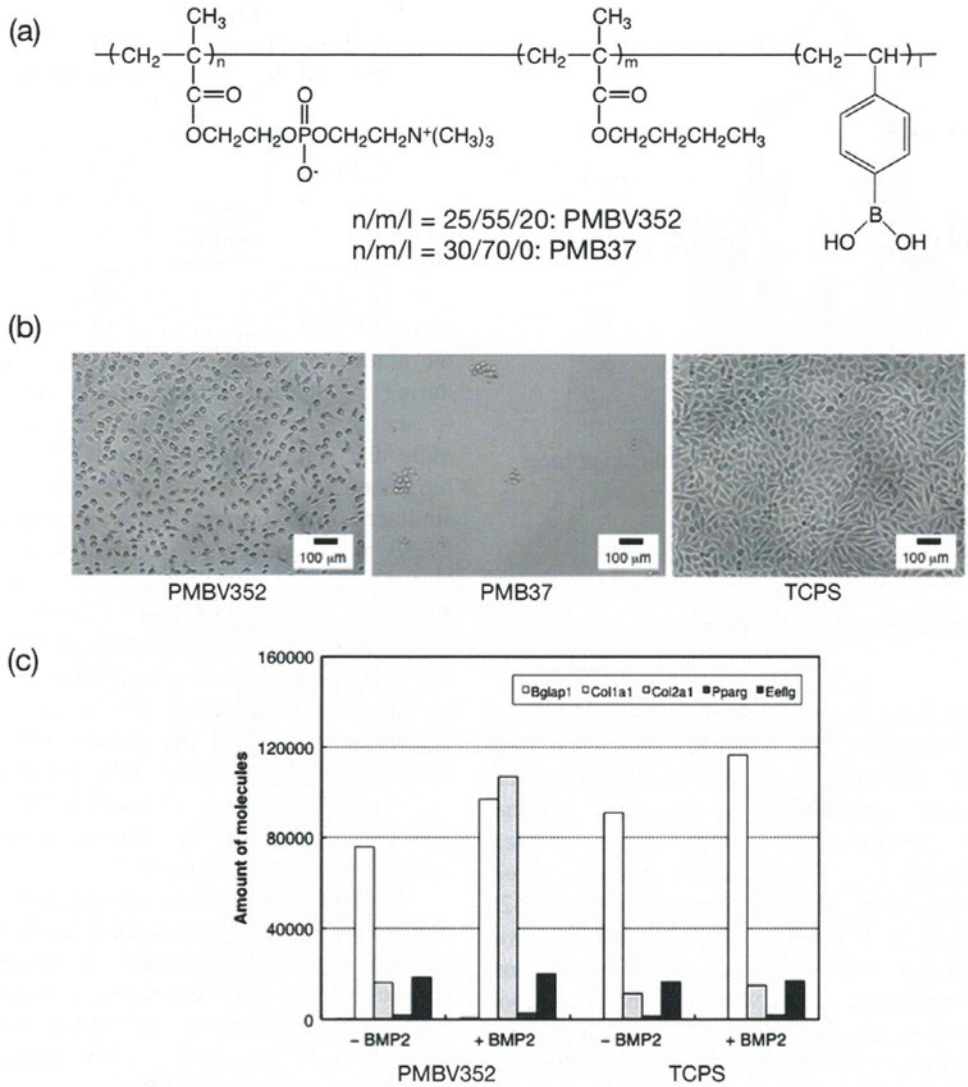

Figure 12. (a) Chemical structure of phospholipid PMBV. (b) Phase-contrast micrographs of adherent L929 cells after 24 h of cultivation on polymer surfaces. The bar corresponds to 100 μm. (c) RT-PCR results showing gene expression in C3H10T1/2 cells grown on polymer surfaces.

membranes [124–129], vascular prostheses [130–133], stents [134, 135], cardiopulmonary bypasses [136–138], and ventricular assist devices (VADs) [139, 140].

Since the first intracoronary stent placement in patients in 1986, mainly for treating acute closure, coronary stenting indications have expanded remarkably. In particular, a drug-eluting stent (DES) is more efficient for reducing in-stent restenosis (ISR) and target lesion revascularization compared with bare metal stents. Because MPC polymers composed of alkyl methacrylates exhibit not only antithrombogenicity but also solute permeability, the polymer is suitable as a coating material for DES. Habara *et al* recently followed up long-term implantation of MPC copolymer-coated stents [141]. Seventy-five patients were treated with MPC copolymer-coated stents for de novo lesions. The data showed that the cumulative major adverse cardiac events (MACE)-free survival rate after 6 months, 18 months and 8 years was 86.3, 83.6 and 78.6%, respectively, without occurrence of thrombosis. The safely of MPC polymer-coated, small-diameter (< 2 mm) stents was also evaluated by Grenadier and coworkers [142].

Some articles described the advantages of MPC polymer coating on cardiopulmonary bypass (CPB) devices for improving the preservation of platelet count and reducing the expression of proinflammatory cytokines in cardiac surgery [137, 138]. The enhanced biocompatibility of MPC polymer-coated circuits can also be combined with other anti-inflammatory strategies.

Titanium alloys are the most common base materials in the latest VADs. VADs provide circulatory support to patients in late-stage heart failures via pulsatile or rotary blood pumps. Unfortunately, VAD implantation is associated with a number of complications including infection, bleeding and thromboembolism. The concerns over biocompatibility may be a major reason why VADs are underutilized in patients with heart failure [143]. In particular, platelet adhesion and thrombus formation occur on titanium surfaces, resulting in the risk of thromboembolism or increased bleeding due to the

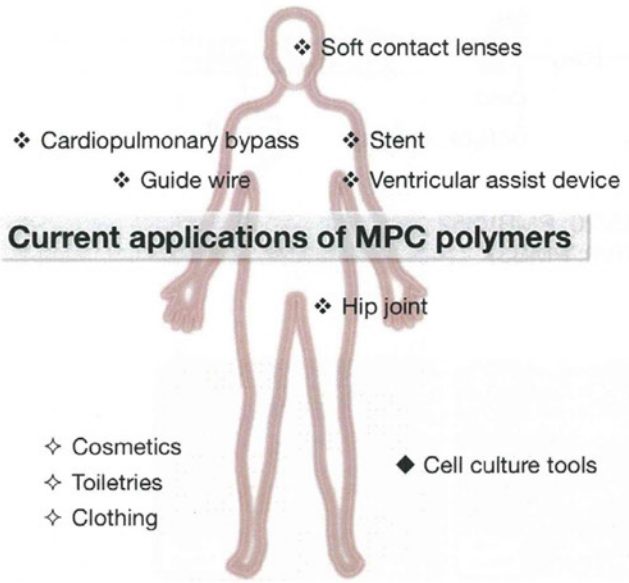

Figure 13. Biomedical and life science applications of MPC polymers.

use of anticoagulants in these patients. To improve the blood compatibility of titanium alloy surfaces, they have been coated with MPC polymers [144]. Snyder and coworkers assessed the blood compatibility of the MPC polymer (PMB37)-coated EVAHEART® VAD (Sun Medical Technology Research Co., Suwa, Japan), through animal testing (figure 14(a)) [145, 146]. Circulating platelet CD62P expression and annexin V binding were significantly lower in animals receiving MPC polymer-coated components compared with components coated with diamond-like carbon (DLC), starting from day 21 and 24 after the operation, respectively, as shown in figure 14(b). Figure 14(c) shows an EVAHEART® VAD explant, coated with an MPC polymer, 34 days after operation. The pump had no anticoagulation treatment, yet no significant thrombus formation was observed.

In May 2005, the first clinical implantation of an EVAHEART® was successfully performed in a pilot study. EVAHEART® is an implantable centrifugal blood pump made from pure titanium; it is sized 55 × 64 mm, and weighs 420 g [147]. In Japan, the cost of the EVAHEART® has been covered by the National Health Insurance since March 2011. A clinical trial of the EVAHEART® has been started in the United States.

4.2. Orthopedic devices

Synovia (or synovial fluid) is a clear, thixotropic, lubricating fluid secreted by membranes in joint cavities, tendon sheaths and bursae, which maintains lubricity in body joints. It contains sugar, proteins and lipids. It is important for reconstruction of joint functions to secure the same lubricous state as in a living body joint. In this section, we examine the method of developing and making the neutral phosphatide of artificial synovia and achieving lubricity; the artificial synovia contains the same ingredients as living body synovia and is adsorbed on the surface of an artificial joint.

Foy *et al* reported that MPC polymers were useful for improving the surface lubrication of polymeric materials under wet conditions [148]. As a result of surface-initiated graft polymerization of MPC, surfaces exhibiting ultralow friction have been obtained. Ishihara *et al* explored a new methodology, namely photoinduced polymerization of MPC on a polyethylene surface [59]. A water-insoluble photoinitiator, benzophenone, was coated on a polyethylene substrate from an acetone solution. The substrate was then exposed to UV light in an MPC aqueous solution. MPC polymerization was initiated on the polyethylene surface, and the molecular weight of the poly(MPC) has been monitored during the irradiation. Moro *et al* applied this technique to the surface modification of a crosslinked ultrahigh molecular weight polyethylene (CLPE) cup of an artificial hip joint [149]. The surface showed high lubricity, which was similar to fluidic friction. The wear of the poly(MPC)-grafted CLPE was significantly reduced compared with that of bare CLPE and of CLPE grafted with other hydrophilic polymers, as shown in figure 15 [150, 151]. Furthermore, the PMPC-modified polyethylene particles did not stimulate osteoclast cells, whereas non-modified polyethylene particles generated from friction and wear of artificial joints did induce osteolysis in artificial hip joints [149]. Very recently, an innovative hip joint system with poly(MPC)-grafted CLPE cup Aquala® (Kyocera Medical Co. Ltd, Osaka, Japan) was approved in Japan; the hip joint is expected to last longer than conventional artificial hip joints.

Kyomoto *et al* reported self-initiated surface grafting with poly(MPC) on poly(ether-ether-ketone) (PEEK) [60, 152], which is a group of polymeric biomaterials with excellent mechanical properties and chemical stability. Benzophenone units were included in the PEEK molecules and then radicals were generated by UV irradiation. The PEEK specimens were soaked in MPC aqueous solution, after which photoinduced graft polymerization was performed at 60 °C for 90 min. The PMPC graft chains were generated on the PEEK surface without reducing mechanical properties of the specimens. Lately, PEEK has emerged as the leading high-performance thermoplastic candidate for replacing metal implant components, especially in the fields of orthopedics and trauma surgery. The improved nonfouling, hydrophilic, and lubricant properties of PEEK with MPC may widen the biomedical applications of PEEK.

4.3. Ophthalmology devices

The soft contact lens (SCL) is one of the most representative products of hydrogel application; it was first introduced in 1961 using poly(2-hydroxyethyl methacrylate). Since then, various poly(2-hydroxyethyl methacrylate)-based hydrogels were developed to improve lens properties. Both oxygen permeability and wettability are required for an SCL, and MPC is a suitable monomer. Biocompatible Co. Ltd (UK) has produced MPC polymer-based SCLs containing 20% of MPC (Proclear®, omafilcon A), which are now commercially available from CooperVision [153]. Recently, silicone hydrogels have been used as base materials for SLC because of their high oxygen permeability. Silicone

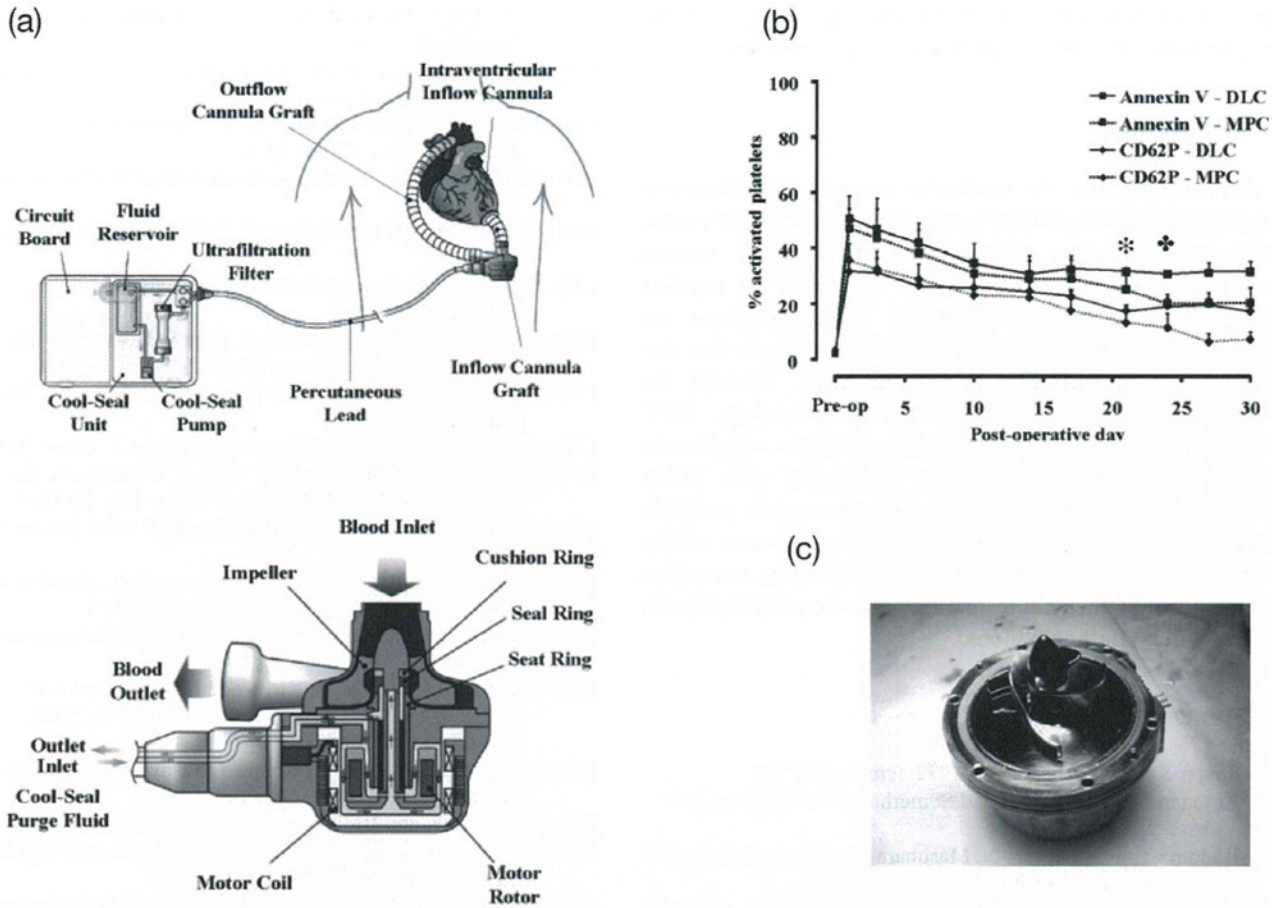

Figure 14. (a) EVAHEART VAD in the preferred anatomic placement for left ventricular support. The system consists of the inflow cannula, pump, outflow cannula, and lubricating purge system. The Cool-Seal purge system consists of a pump, ultrafiltration filter, and reservoir contained in a small case that can be carried by the patient. Water is recirculated through the system by the Cool-Seal pump, the ultrafiltration unit ensures sterility of fluid egressing the unit to the blood pump, and the reservoir can be exchanged or refilled as needed. (b) The concentrations of circulating activated platelets as quantified by annexin V binding or CD62P expression are shown for DLC-coated ($N = 4$) and MPC polymer-coated ($N = 16$) components. The days when the MPC values become significantly lower than the DLC values for annexin V (❊) and CD62P (✤) are marked above the curves. (c) Pump (MPC polymer coating) after 34 days of support without anticoagulation treatment. (Reprinted from [146, 147] with permission from Wiley.)

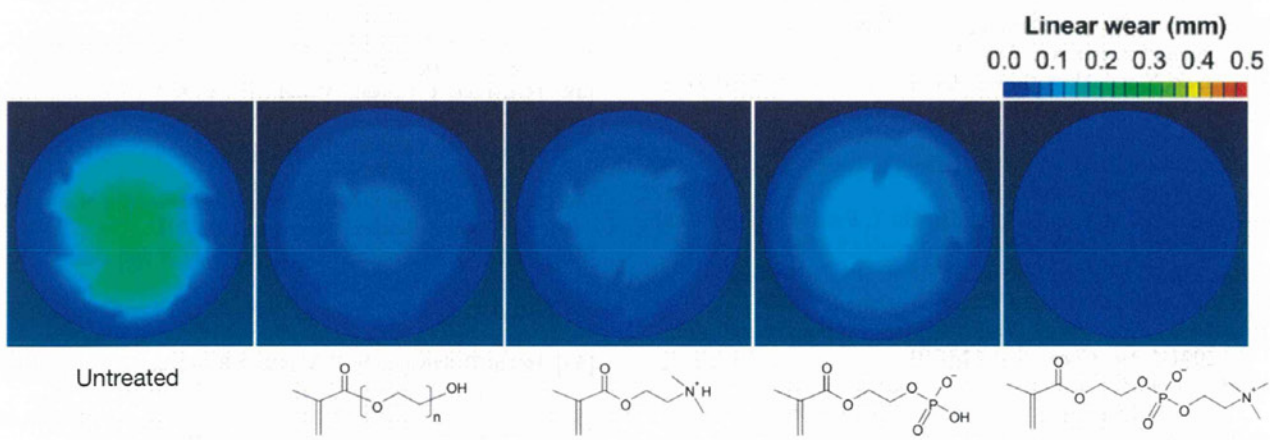

Figure 15. Spatial maps of wear in CLPE cups grafted with poly(MPC) or other polyelectrolytes after a hip simulator test.

hydrogels are normally prepared by copolymerization of macromonomers bearing silicone and hydrophilic monomers. The wettability of the silicone hydrogels is sometimes not adequate to provide the wearer with a comfortable feeling. MPC polymers have been developed for coatings to improve the surface wettability of silicone hydrogels; the surfaces also show good antifouling properties. Through the formation of interpenetrating poly(MPC) networks, Ishihara

and co-workers have succeeded in preparing superhydrophilic silicone hydrogels with a high degree of transparency [52].

5. Conclusions

In this review article, the molecular design and fundamental properties of cell membrane-inspired phospholipid polymers, MPC polymers, are summarized. In addition, surface modification processes using MPC polymers to regulate biological responses are described. MPC polymers are suitable for preparing not only nonfouling surfaces but also platforms of biomolecules and living cells. Through the combination of nanotechnology and biotechnology, MPC polymer science has made considerable progress with devices such as biosensors, biochips and bioimaging tools [154]. MPC and various kinds of MPC polymers are now available commercially worldwide, and many medical devices treated with MPC polymers are used in clinics. Therefore, we expect that the novel biomedical technology based on MPC polymer science will be further explored.

References

[1] Singer S J and Nicolson G L 1972 *Science* **175** 723
[2] Virtanen J A, Cheng K H and Somerharju P 1998 *Proc. Natl Acad. Sci. USA* **95** 4964
[3] Kadoma Y, Nakabayashi N, Masuhara E and Yamauchi J 1978 *Koubunshi Ronbunshu* **35** 423 (in Japanese)
[4] Ishihara K, Ueda T and Nakabayashi N 1990 *Polym. J.* **22** 355
[5] Ueda T, Oshida H, Kurita K, Ishihara K and Nakabayashi N 1992 *Polym. J.* **24** 1259
[6] Inoue Y, Watanabe J, Takai M and Ishihara K 2004 *J. Biomater. Sci. Polym. Edn.* **15** 1153
[7] Ma Y, Tang Y, Billingham N C, Armes S P, Lewis A L, Lloyd A W and Salvage J P 2003 *Macromolecules* **36** 3475
[8] Ma Y, Tang Y, Billingham N C, Armes S P and Lewis A L 2003 *Biomacromolecules* **4** 864
[9] Li Y, Armes S P, Jin X and Zhu S 2003 *Macromolecules* **36** 8268
[10] Ishihara K, Tsuji T, Kurosaki K and Nakabayashi N 1994 *J. Biomed. Mater. Res.* **28** 225
[11] Iwasaki Y and Akiyoshi K 2004 *Macromolecules* **37** 7637
[12] Watanabe J, Eriguchi T and Ishihara K 2002 *Biomacromolecules* **3** 1109
[13] Watanabe J, Eriguchi T and Ishihara K 2002 *Biomacromolecules* **3** 1375
[14] Samanta D, McRae S, Cooper B, Hu Y, Emrick T, Pratt J and Charles S A 2008 *Biomacromolecules* **9** 2891
[15] Ishihara K 2012 *Encyclopedia Polym. Sci. Tech.* at press
[16] Kiritoshi Y and Ishihara K 2004 *Polymer* **45** 7499
[17] Lobb E J, Ma I, Billingham N C, Armes S P and Lewis A L 2001 *J. Am. Chem. Soc.* **123** 791
[18] Ma I, Lobb E J, Billingham N C, Armes S P, Lewis A L, Lloyd A W and Salvage J 2002 *Macromolecules* **35** 9306
[19] Madsen J, Warren N J, Armes S P and Lewis A L 2011 *Biomacromolecules* **12** 2225
[20] Seo J H, Matsuno R, Lee Y, Takai M and Ishihara K 2009 *Biomaterials* **30** 4859
[21] Chen X, McRae S, Samanta D and Emrick T 2010 *Macromolecules* **43** 6261
[22] Xu J P, Ji J, Chen W D and Shen J C 2005 *Macromol. Biosci.* **5** 164
[23] Iwasaki Y and Akiyoshi K 2006 *Biomacromolecules* **7** 1433
[24] Li Y, Tang Y, Narain R, Lewis A L and Armes S P 2005 *Langmuir* **21** 9946
[25] Yusa S, Fukuda K, Yamamoto T, Ishihara K and Morishima Y 2005 *Biomacromolecules* **6** 663
[26] Bhuchar N, Thundat T, Sunasee R, Ishihara K and Narain R 2012 *Bioconjug. Chem.* **23** 75
[27] Bhuchar N, Deng Z, Ishihara K and Narain R 2011 *Polym. Chem.* **2** 623
[28] Yu B, Lowe A B and Ishihara K 2009 *Biomacromolecules* **10** 950
[29] Yuan J J, Schmid A, Armes S P and Lewis A L 2006 *Langmuir* **22** 11022
[30] Akkahat P, Kiatkamjornwong S, Yusa S, Hoven V P and Iwasaki Y 2012 *Langmuir* **28** 5872
[31] Iwasaki Y, Matsumoto A and Yusa S 2012 *ACS Appl. Mater. Interfaces* **4** 3254
[32] Iwasaki Y and Ishihara K 2005 *Anal. Bioanal. Chem.* **381** 534
[33] Ishihara K, Oshida H, Endo Y, Ueda T, Watanabe A and Nakabayashi N 1992 *J. Biomed. Mater. Res.* **26** 1543
[34] Ishihara K, Iwasaki Y and Nakabayashi N 1999 *Polym. J.* **31** 1231
[35] Yamasaki A, Imamura Y, Kurita K, Iwasaki Y, Nakabayashi N and Ishihara K 2003 *Colloid. Surf.* B **28** 53
[36] Iwasaki Y, Yamasaki A and Ishihara K 2003 *Biomaterials* **24** 3599
[37] Lewis A L, Hughes P D, Kirkwood L C, Leppard S W, Redman R P, Tolhurst L A and Stratford P W 2000 *Biomaterials* **21** 1847
[38] Futamura K, Matsuno R, Konno T, Takai M and Ishihara K 2008 *Langmuir* **24** 10340
[39] Fukazawa K and Ishihara K 2012 *Colloid. Surf.* B **97** 70
[40] Iwasaki Y, Takamiya M, Iwata R, Yusa S and Akiyoshi K 2007 *Colloid. Surf.* B **57** 226
[41] Choi J, Konno T, Takai M and Ishihara K 2012 *Biomaterials* **33** 954
[42] Choi J, Konno T, Matsuno R, Takai M and Ishihara K 2008 *Colloid. Surf.* B **67** 216
[43] Pang S, Zhu C, Xu F, Chen C and Ji J 2012 *Colloid. Surf.* B **94** 22
[44] Ishihara K, Hanyuda H and Nakabayashi N 1995 *Biomaterials* **16** 873
[45] Ishihara K, Shibata N, Tanaka S, Iwasaki Y, Kurosaki T and Nakabayashi N 1996 *J. Biomed. Mater. Res.* **32** 401
[46] Yoneyama T, Ishihara K, Nakabayashi N, Ito M and Mishima Y 1998 *J. Biomed. Mater. Res.* **43** 15
[47] Ishihara K, Fukumoto K, Iwasaki Y and Nakabayashi N 1999 *Biomaterials* **20** 1545
[48] Hasegawa T, Iwasaki Y and Ishihara K 2001 *Biomaterials* **22** 243
[49] Ishihara K, Nishiuchi D, Watanabe J and Iwasaki Y 2004 *Biomaterials* **25** 71
[50] Iwasaki Y, Aiba Y, Morimoto N, Nakabayashi N and Ishihara K 2000 *J. Biomed. Mater. Res.* **52** 701
[51] Morimoto N, Iwasaki Y, Nakabayashi N and Ishihara K 2002 *Biomaterials* **23** 4881
[52] Shimizu T, Goda T, Minoura N, Takai M and Ishihara K 2010 *Biomaterials* **31** 3274
[53] Hoshi T, Sawaguchi T, Matsuno R, Konno T, Takai M and Ishihara K 2012 *J. Mater. Chem.* **20** 4897
[54] Hoshi T, Sawaguchi T, Matsuno R, Konno T, Takai M and Ishihara K 2008 *J. Supercritical Fluids* **44** 391
[55] Ishihara K, Fukumoto K, Aoki J and Nakabayashi N 1992 *Biomaterials* **13** 145
[56] Ishihara K, Miyazaki H, Kurosaki T and Nakabayashi N 1995 *J. Biomed. Mater. Res.* **29** 181
[57] Hsiue G H, Lee S D, Chang P C T and Kao C Y 1998 *J. Biomed. Mater. Res.* **42** 134
[58] Iwasaki Y, Sawada S, Nakabayashi N, Khang G, Lee H B and Ishihara K 1999 *Biomaterials* **20** 2185

[59] Ishihara K, Iwasaki Y, Ebihara S, Shindo Y and Nakabayashi N 2000 *Colloid. Surf.* B **18** 325
[60] Kyomoto M and Ishihara K 2009 *ACS Appl. Mater. Interf.* **1** 537
[61] Feng W, Brash J and Zhu S P 2004 *J. Polym. Sci. A: Polym. Chem.* **42** 2931
[62] Iwata R, Suk-In P, Hoven V P, Takahara A, Akiyoshi K and Iwasaki Y 2004 *Biomacromolecules* **5** 2308
[63] Feng W, Zhu S, Ishihara K and Brash J L 2005 *Langmuir* **21** 5980
[64] Tsujii Y, Ohno K, Yamamoto S Goto A and Fukuda T 2006 *Adv. Polym. Sci.* **197** 1
[65] Ishihara K, Nomura H, Mihara T, Kurita K, Iwasaki Y and Nakabayashi N 1998 *J. Biomed. Mater. Res.* **39** 323
[66] Konno K, Watanabe J and Ishihara K 2004 *Biomacromolecules* **5** 342
[67] Kinoshita K *et al* 2006 *Nucleic Acids Res.* **35** e3
[68] Iwata R, Sato R, Iwasaki Y and Akiyoshi K 2008 *Colloid. Surf.* B **62** 288
[69] Chantasirichot S and Ishihara K 2012 *Biosens. Bioelectron.* **38** 209
[70] Watanabe J and Ishihara K 2006 *Biomacromolecules* **7** 171
[71] Watanabe J and Ishihara K 2007 *Nanobiotechnology* **3** 76
[72] Goto Y, Matsuno R, Konno T, Takai M and Ishihara K 2008 *Biomacromolecules* **9** 3252
[73] Ishihara K, Goto Y, Matsuno R, Inoue Y and Konno T 2012 *Biochim. Biophys. Acta* **1810** 268
[74] Matsuno R and Ishihara K 2011 *Nano Today* **6** 61
[75] Ishihara K, Aragaki R, Ueda T, Watanabe A and Nakabayashi N 1990 *J. Biomed. Mater. Res.* **24** 1069
[76] Ishihara K, Ziats N P, Tierney B P, Nakabayashi N and Anderson J M 1991 *J. Biomed. Mater. Res.* **25** 1397
[77] Ishihara K, Oshida H, Endo Y, Watanabe A, Ueda T and Nakabayashi N 1993 *J. Biomed. Mater. Res.* **27** 1309
[78] Zhang S, Benmakroha , Rolf P, Tanaka S and Ishihara K 1996 *Biosens. Bioelectron.* **11** 1019
[79] Fujii K, Matsumoto H N, Koyama Y, Iwasaki Y, Ishihara K and Takakuda K 2008 *J. Vet. Med. Sci.* **70** 167
[80] Nakai K, Morigaki K and Iwasaki Y 2010 *Soft Matter* **6** 5937
[81] Iwasaki Y, Mikami A, Kurita K, Ishihara K and Nakabayashi N 1997 *J. Biomed. Mater. Res.* **36** 508
[82] Matyjaszewski K and Xia J 2001 *Chem. Rev.* **101** 2921
[83] Matyjaszewski K *et al* 1999 *Macromolecules* **32** 8716
[84] Kong X, Kawai T, Abe J and Iyoda T 2001 *Macromolecules* **34** 1837
[85] Huang W, Kim J B, Bruening M L and Baker G L 2002 *Macromolecules* **35** 1175
[86] Shah R R, Merreceyes D, Husemann M, Rees I, Abbott N L, Hawker C J and Hedrick J L 2000 *Macromolecules* **33** 597
[87] Jones D M and Huck W T S 2001 *Adv. Mater.* **13** 1256
[88] Tsujii Y, Ejaz M, Yamamoto S, Fukuda T, Shigeto K, Mibu K and Shinjo T 2002 *Polymer* **43** 3837
[89] Maeng I S and Park J W 2003 *Langmuir* **19** 9973
[90] Inoue Y, Nakanishi T and Ishihara K 2011 *React. Funct. Polym.* **71** 350
[91] Feng W, Brash J L and Zhu S 2006 *Biomaterials* **27** 847
[92] Yoshimoto K, Hirase T, Madsen J, Armes S P and Nagasaki Y 2009 *Macromol. Rapid. Commun.* **30** 2136
[93] Kobayashi M, Yamaguchi H, Terayama Y, Wang Z, Ishihara K, Hino M and Takahara A 2009 *Macromol. Symp.* **279** 79
[94] Kobayashi M and Takahara A 2010 *Chem. Rec.* **10** 208
[95] Iwasaki Y, Sawada S, Ishihara K, Khang G and Lee H B 2002 *Biomaterials* **23** 3897
[96] Sawada S, Sakaki S, Iwasaki Y, Nakabayashi N and Ishihara K 2003 *J. Biomed. Mater. Res.* A **64** 411
[97] Pricer W E, Hudgin R L, Ashwell G, Stockert R J and Morell A G 1974 *Methods Enzymol.* **34** 688
[98] Stockert R J 1995 *Physiol. Rev.* **75** 591
[99] Weigel P H, Scnnaar R L, Kuhlenschmidt M S, Schmell E, Lee R T, Lee Y C and Roseman S 1979 *J. Biol. Chem.* **254** 10830
[100] Kobayashi A, Akaike T, Kobayashi K and Sumitomo H 1986 *Makromol. Chem., Rapid Commun.* **7** 645
[101] Gutsche A T, Parsons-Wingerter P, Chand D, Saltzman W M and Leong K W 1994 *Biotechnol. Bioeng.* **43** 801
[102] Sagara K and Kim S W 2002 *J. Control. Release* **79** 271
[103] Kim S H, Hoshiba T and Akaike T 2004 *Biomaterials* **25** 1813
[104] Sato K, Miura Y, Saito N, Kobayashi K and Takai O 2007 *Biomacromolecules* **8** 753
[105] Yarema K J, Mahal L K, Bruehl R E, Rodriguez E C and Bertozzi C R 1998 *J. Biol. Chem.* **273** 31168
[106] Iwasaki Y, Takami U, Shinohara U, Kurita K and Akiyoshi K 2007 *Biomacromolecules* **8** 2788
[107] Barrera D A, Zylstra E, Lansbury P and Langer R 1995 *Macromolecules* **28** 425
[108] Vunjak-Novakovic G, Obradovic B, Martin I, Bursac P M, Langer R and Freed L E 1998 *Biotechnol. Prog.* **14** 193
[109] Ishaug-Riley S L, Crane-Kruger G M, Yaszemski M J and Mikos A G 1998 *Biomaterials* **19** 1405
[110] Wald L, Sarakinos A G, Lyman M D, Mikos A G, Vacanti J P and Langer R 1993 *Biomaterials* **14** 270
[111] Iwasaki Y, Sawada S, Ishihara K, Khang G and Lee H B 2002 *Biomaterials* **23** 3897
[112] Liu C, Long L, Li Z, He B, Wang L, Wang J, Yuan X and Sheng J 2012 *J. Microencapsul.* **29** 242
[113] Saito A, Konno T, Ikake H, Kurita K and Ishihara K 2010 *Biomed. Mater.* **5** 054101
[114] Konno T and Ishihara K 2007 *Biomaterials* **28** 1770
[115] Xu Y, Jang K, Yamashita T, Tanaka Y, Mawatari K and Kitamori T 2012 *Anal. Bioanal. Chem.* **402** 99
[116] Xu Y, Sato K, Mawatari K, Konno T, Ishihara K and Kitamori T 2010 *Adv. Mater.* **22** 3017
[117] Kitano S, Koyama Y, Kataoka K, Okano T and Sakurai Y 1992 *J. Control. Release* **19** 161
[118] James T D, Sandanayake K R A S and Shinkai S 1994 *Angew. Chem., Int. Ed.* **33** 2207
[119] Miyata T, Uragami T and Nakamae K 2002 *Adv. Drug Deliv. Rev.* **54** 79
[120] Aikawa T, Konno T, Takai M and Ishihara K 2012 *Langmuir* **28** 2145
[121] Ishihara K 2000 *Sci. Technol. Adv. Mater.* **1** 131
[122] Iwasaki Y, Ishihara K and Nakabayashi N 1997 *Recent Res. Dev. Polym. Sci.* **1** 37
[123] Ishihara K 1997 TRIP **5** 401
[124] Hasegawa T, Iwasaki Y and Ishihara K 2002 *J. Biomed. Mater. Res.* **63** 333
[125] Iwasaki Y, Nakabayashi N and Ishihara K 2003 *J. Artif. Organs* **6** 260
[126] Ye S H, Watanabe J, Takai M, Iwasaki Y and Ishihara K 2005 *Biomaterials* **26** 5032
[127] Dahe G J, Kadam S S, Sabale S S, Kadam D P, Sarkate L B and Bellare J R 2011 *PLoS One* **6** e25236
[128] Ueda H, Watanabe J, Konno T, Takai M, Saito A and Ishihara K 2006 *J. Biomed. Mater. Res.* A **77** 19
[129] Myers G J, Johnstone D R, Swyer W J, McTeer S, Maxwell S L and Squires C 2003 *J. Extra Corpor. Technol.* **35** 6
[130] Yoneyama T, Ishihara K, Nakabayashi N, Ito M and Mishima Y 1998 *J. Biomed. Mater. Res.* **43** 15
[131] Yoneyama T, Ito M, Sugihara K, Ishihara K and Nakabayashi N 2000 *Artif. Organs* **24** 23
[132] Yoneyama T, Sugihara K, Ishihara K, Iwasaki Y and Nakabayashi N 2002 *Biomaterials* **23** 1455
[133] Soletti L, Nieponice A, Hong Y, Ye S H, Stankus J J, Wagner W R and Vorp D A 2011 *J. Biomed. Mater. Res.* A **96** 436

[134] Lewis A L, Furze J D, Small S, Robertson J D, Higgins B J, Taylor S and Ricci D R 2002 *J. Biomed. Mater. Res.* **63** 699
[135] Lewis A L, Willis S L, Small S A, Hunt S R, O'Byrne V and Stratford P W 2004 *Biomed. Mater. Eng.* **14** 355
[136] Iwasaki Y, Uchiyama S, Kurita K, Morimoto N and Nakabayashi N 2002 *Biomaterials* **23** 3421
[137] De S F, Van B Y, Caes F, François K, Arnout J, Bossuyt X, Taeyans Y and Van N G 2002 *Perfusion* **17** 39
[138] Schulze C J, Han L, Ghorpade N, Etches W S, Stang L, Koshal A and Wang S H 2009 *J. Card. Surg.* **24** 363
[139] Yamazaki K, Kihara S, Akimoto T, Tagusari O, Kawai A, Umezu M, Tomioka J, Kormos R L, Griffith B P and Kurosawa H 2002 *Japan J. Thorac. Cardiovasc. Surg.* **50** 461
[140] Kitao T *et al* 2011 *Artif. Organs* **35** 543
[141] Habara S *et al* 2011 *Int. Heart J.* **52** 88
[142] Grenadier E, Roguin A, Hertz I, Peled B, Boulos M, Nikolsky E, Amikam S, Kerner A, Cohen S and Beyar R 2002 *Catheter Cardiovasc. Interv.* **55** 303
[143] Deng M C, Edwards L B, Hertz M I, Rowe A W, Keck B M, Kormos R L, Naftel D C, Kirklin J K and Taylor D O 2005 *J. Heart Lung Transplant.* **24** 1182
[144] Ye S H, Johnson C A Jr, Woolley J R, Snyder T A, Gamble L J and Wagner W R 2009 *J. Biomed. Mater. Res.* A **91** 18
[145] Kihara S *et al* 2003 *Artif. Organs* **27** 188
[146] Snyder T A, Tsukui H, Kihara S, Akimoto T, Litwak K N, Kameneva M V, Yamazaki K and Wagner W R 2007 *J. Biomed. Mater. Res.* A **81** 85
[147] Yamazaki K, Saito S, Kihara S, Tagusari O and Kurosawa H 2007 *Gen. Thorac. Cardiovasc. Surg* . **55** 158
[148] Foy J R, Williams P F III, Powell G L, Ishihara K, Nakabayashi N and LaBerge M 1999 *Proc. Inst. Mech. Eng.* H **213** 5
[149] Moro T, Takatori Y, Ishihara K, Konno T, Takigawa Y, Matsushita T, Chung U I, Nakamura K and Kawaguchi H 2004 *Nat. Mater.* **3** 829
[150] Kyomoto M, Moro T, Konno T, Takadama H, Yamawaki N, Kawaguchi H, Takatori Y, Nakamura K and Ishihara K 2007 *J. Biomed. Mater. Res.* A **82** 10
[151] Kyomoto M, Moro T, Saiga K, Hashimoto M, Ito H, Kawaguchi H, Takatori Y and Ishihara K 2012 *Biomaterials* **33** 4451
[152] Kyomoto M, Moro T, Takatori Y, Kawaguchi H, Nakamura K and Ishihara K 2010 *Biomaterials* **31** 1017
[153] Goda T and Ishihara K 2006 *Expert Rev. Med. Devices* **3** 167
[154] Lewis A L and Lloyd A W 2012 *Biomimetic, Bioresponsive, Bioactive Materials: An Introduction to Integrating Materials with Tissues* ed M Santin and G J Phillips (Hoboken, NJ: Wiley) p 95

Trans. Mat. Res. Soc. Japan 37[3] 333-336 (2012)

Effects of dynamics of water molecules at hydrophilic polymer brush surfaces on protein adsorption behavior

Kazuomi Inoue[1], Yuuki Inoue*[1,3], and Kazuhiko Ishihara[1,2,3]

[1] Department of Materials Engineering, [2] Department of Bioengineering, School of Engineering, The University of Tokyo, Tokyo 113-8656, Japan,

[3] JST-CREST, Tokyo 102-0075, Japan

E-mail: inoue@mpc.t.u-tokyo.ac.jp

The suppression of protein adsorption must be required for a surface of biomaterials to avoid undesirable biological reactions. Understanding the interactions between proteins and surfaces is necessary to construct new biomaterials that have ultimate nonbiofouling property. Protein adsorption causes in an aqueous medium, therefore, we focused on the hydration state at the interface of the aqueous medium with proteins and the contacting materials, and investigated the effects of hydration state on protein adsorption behavior towards the surface. We could successfully establish the method for evaluation of dynamics of water molecules in the vicinity of the surface by using proton nuclear magnetic resonance spectroscopy for the hydrated polymer brush layer-modified micro-silica beads. The zwitterionic and cationic polymer brush surfaces were used for the measurement. The results clearly indicated that the dynamics of water molecules determined protein adsorption onto the surfaces. Thus, the polymer brush surfaces with hydration layer and high-diffusion of water molecules in the layer, such as phosphorylcholine group-bearing polymer brush surface, were effective to inhibit protein adsorption.

Key words: dynamics of water, protein adsorption, polymer brush structure, nuclear magnetic resonance, relaxation time

1. INTRODUCTION

Biological reactions, which are induced at a surface of materials when they contact with blood and tissues, such as thrombus formation, immunoresponse, and inflammatoric response, are initiated by protein adsorption on the surface [1]. Therefore, biomaterials surface requires quite strong inhibition for protein adsorption. The proteins interact with the materials surface by combination of various molecular forces generated in an aqueous medium. There is a hypothesis that shows protein adsorption would be caused by hydration layer with low motility [2]. In this regard, dynamics of water should be considered in order to realize zero protein adsorption surface. Some reports have attempted to clarify hydration state, and it was revealed that hydration state at the surface has strong effect on protein adsorption [3-8]. Among them, Ishihara *et al.* clearly demonstrated that the hydrophilic polymer surfaces with high-free water fraction reduced protein adsorption. That is, when the free-water fraction became up to 0.7, amount of protein adsorbed on the surface reduces below monolayer adsorption [3]. However, the role of water molecules at the protein-material interface is only guessed from static information of bulk water. Also, these previous reports were conducted using polymer coated surfaces, which have other difficulties for evaluation of water dynamics due to entanglement of polymer chains and entrapment of water molecules physically in the hydrated layer. From these points of view, we applied well-defined polymer brush surface with the controlled density and thickness of the polymer layer. The goal of this study is to understand the dynamics of water molecules focusing on the surface.

In this study, water that is coexisted with polymer chains in extended nanometer-space was acquired by using micro-silica beads covered with polymer brush layers [9, 10]. High-density polymer brush layers with various chemical structures were prepared on the micro-silica beads via surface-initiated atom transfer radical polymerization (SI-ATRP) [11]. Hydration state at the surfaces was evaluated by measurement of

relaxation time and diffusion coefficient using proton nuclear magnetic resonance spectroscopy (^{1}H-NMR) [12, 13]. Protein adsorption onto the surfaces was measured with a quartz crystal microbalance with dissipation monitoring (QCM-D) measurement [14, 15]. Finally, the relationship between protein adsorption and dynamics of water was discussed.

2. EXPERIMENTS

2.1. Materials

Three kinds of zwitterionic monomers and cationic one were used for making polymer brush surface. 2-Methacryloyloxyethyl phosphorylcholine (MPC) was synthesized and purified using a previously reported method [16]. [2-(Methacryloyloxy) ethyl] dimethyl (3-sulfopropyl) ammonium hydroxide (SBMA) was purchased from Sigma-Aldrich Co. (St. Louis, USA). *N*-Methacryloyloxyethyl *N*, *N*-dimethyl ammonium -α-*N*-methyl carboxylate (CBMA) was obtained from Wako Pure Chemistry (Osaka, Japan). Trimethyl-2-methacroyloxyethylammonium Chloride (TMAEMA) was purchased from Tokyo Chemical Industry Co., Ltd. (Tokyo, Japan). Copper (I) bromide (CuBr), 2,2'-bipyridyl (bpy), and ethyl-2-bromoisobutyrate (EBIB) were purchased from Sigma–Aldrich Co. and were directly used as received. All other reagents and solvents of extra-pure grade were commercially available and were directly used as purchased. Micro-silica beads with 10-μm in diameter were purchased from Fuji Silysia Chemical Ltd. (Aichi, Japan).

2.2. Preparation of initiator immobilized beads

The surface-immobilizing initiator for SI-ATRP, (11-(2-bromo-2-methyl) propionyloxy) undecyltrichlorosilane (BrC10TCS) was synthesized using a previously described method [11, 17]. The micro-silica beads were etched using piranha solution, which is consisted of 30 % of hydrogen peroxide and 70 % of sulfuric acid, for 15 min. The silica beads were removed from the solution and washed with plenty of distilled water. The cleaned silica beads were immersed in a 5 mmol/L solution of BrC10TCS in toluene for 24 h. The BrC10TCS-immobilized silica beads were removed from the solution, rinsed with toluene and methanol, and dried in a dry box under reduced pressure.

2.3. Preparation of polymer brush-modified beads

MPC, SBMA, CBMA, and TMAEMA were graft polymerized from the BrC10TCS-immobilized silica beads using SI-ATRP as follows: CuBr, bpy, and each monomer in a particular molar ratio were placed in a glass tube and dehydrated; thereafter, degassed solvents were added into the glass tube. The following solvents were used: ethanol for MPC and CBMA at a monomer concentration of 0.56 mol/L, a mixture of methanol and water (50:50 by volume %) for SBMA at a monomer concentration of 0.38 mol/L, and a mixture of methanol and water (70:30 by volume %) for TMAEMA at a monomer concentration of 1.0 mol/L. Sodium chloride of the same concentration as SBMA (0.38 mol/L) was added to the SBMA solution to prevent the precipitation of poly(SBMA) during polymerization. Argon was bubbled into each monomer solution at room temperature for 10 min. The BrC10TCS-immobilized silica beads were then immersed into the solution, and EBIB was simultaneously added as the free initiator at one-fiftieth of monomer concentration. After the glass tubes were sealed, polymerization was performed at 20 °C with stirring. After 24 h, the obtained silica beads were removed from the polymerization solution using centrifugation, rinsed with solvents (ethanol for poly(MPC) and poly(CBMA), sodium chloride solution for poly(SBMA), and water for poly(TMAEMA)), and dried in a dry box under reduced pressure. The structure of the polymer brush surface was shown in Fig. 1.

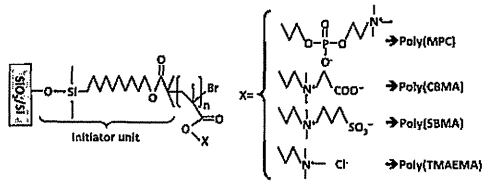

Fig. 1. Chemical structures of polymer brush surface.

2.4. Analysis of hydration state

2.4.1. Measurement of diffusion coefficient

The polymer brush layer-modified silica beads (500 mg) were packed into NMR tubing (ϕ = 10 mm, JEOL, Tokyo, Japan) and distilled water (500 μL) was added into the NMR tubing. Diffusion coefficient (D) measurement of water molecules was performed using ^{1}H-NMR (MU-25, JEOL, Tokyo, Japan) with pulse field gradient method. The D value is an indication of motility of water molecules. The interspaces among the silica beads are extremely small, therefore, we can investigate only water molecules in the vicinity of the polymer brush surface [9, 10].

2.4.2. Evaluation of hydration layer

In order to evaluate the diffusing range of hydrated layers around polymer brush surfaces, relaxation time of water molecules was measured about three types of

samples as followed (Fig. 2). The polymer brush layer-modified silica beads were packed into an NMR tube and distilled and degassed water was added into the tube (type-1). The polymer brush layer-modified silica beads were damped with vapor of saturated sodium chloride solution (RH=75%) and packed into an NMR tube (type-2). Distilled water was degassed with vacuum, and poured into an NMR tube (type-3). Spin-lattice relaxation time (T_1 value) of water molecules was measured using ^{1}H-NMR with inversion recovery method. We defined T_1 for type-1 as T_{1liq}, T_1 for type-2 as T_{1vap}, and T_1 for type-3 as T_{1bulk}, respectively. We presumed that hydration state in liquid water around the polymer brush layer (type-1) would be regarded as a overlap of hydration state of the polymer brush layer only (type-2) and that of a bulk water (type-3). In the case that contains the multi-components of T_1 value, the following equation is generally used [9].

$$1 / T_{1liq} = \alpha / T_{1vap} + (1-\alpha) / T_{1bulk}$$

We hypothesized that the α value would represent the diffusing range of hydrated layers around polymer brush surfaces in liquid water. In this study, the α values were calculated at the several kinds of the polymer brush surface.

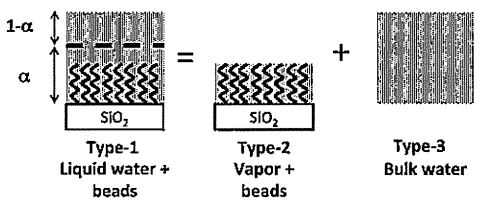

Fig. 2. Samples for evaluation of diffusing range of hydrated layer.

2.5. Protein adsorption measurement

The adsorbed amount of proteins from 100% fetal bovine serum (FBS) on the polymer brush surfaces at 37 °C was quantified using QCM-D measurement (Q-Sense, Gothenburg, Sweden) [14, 15, 17]. To measure the protein adsorption mass on the surface, the polymer brush layers were formed at the surface of QCM-D gold sensor. The following equation was used to estimate the adsorbed amount of protein on the polymer brush surface.

Protein adsorption amount (ng/cm^2) =
17.7 x Frequency shift value (Hz)

3. RESULTS AND DISCUSSION

3.1. Hydration state

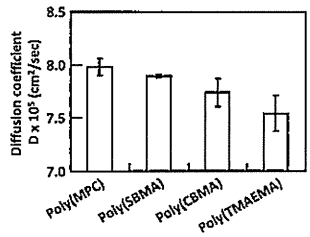

Fig. 3. Diffusion coefficient of water molecules in various hydrated polymer brush system.

Fig. 3 shows the diffusion coefficient (D) values of water at various polymer brush layer-modified silica beads system. The zwitterionic polymer brush surfaces had higher diffusion coefficient compared to the cationic one. In particular, poly(MPC) brush surface had a larger D value. This result means that water molecules near poly(MPC) brush surface has a high motility. On the other hand, the motility of water molecules near poly(TMAEMA) brush surface was restrained. Recently, Takahara *et al.* reports the solubilizing state and dimension of polymer chains in several polymer brush layers in an aqueous medium. In this report, the poly(MPC) chains expanded in the aqueous medium well and the dimension of poly(MPC) chains was not changed by the ionic strength of the aqueous medium [18]. It is well known that the polymer chains shrink in an aqueous medium with ions because the ions would extract water molecules hydrated at polymer chains. The relatively high D value of water molecules and well-expanded structure of the poly(MPC) chains in ionic medium indicated that water molecules may be bounded quite weakly with the poly(MPC) chains.

Fig. 4 shows the diffusing range of hydrated layer (α values) at several polymer brush surfaces. Cationic poly(TMAEMA) surface had larger hydration layer than zwitterionic polymer surfaces. This result can be explained by two effects. First, the poly(TMAEMA) chains expands in an aqueous medium much wider than zwitterionic polymer chains due to strong electrostatic repulsion forces among cationic charges. Second, water molecules strongly hydrated surrounding each poly(TMAEMA) chain [19]. It is difficult to distinguish these effects in the present time, we are now evaluating

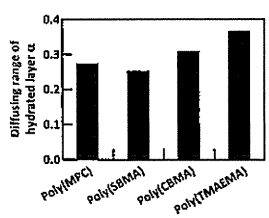

Fig. 4. Diffusing range of hydrated layer at several polymer brush surfaces.

the real number of water molecules bounded on the monomer unit in the polymer chains.

3.2. Relationship between protein adsorption and dynamics of water

As seen in Fig. 5, we determined the relationship between protein adsorption and dynamics of water at the polymer brush surfaces. The polymer brush surface with larger diffusion coefficient resisted protein adsorption. Particularly, large amount of protein adsorbed on poly(TMAEMA) brush surface. Compared to the theoretical monolayer adsorption mass, the multilayer adsorption would occur on the cationic polymer brush surface. The multilayer adsorption would be promoted at the cationic surface because of both electrostatic interaction and its thick hydration layer with lower motility of water molecules around the cationic surface. These effects would be due to the outstanding difference in protein adsorption mass between on the cationic surface and zwitterionic surfaces.

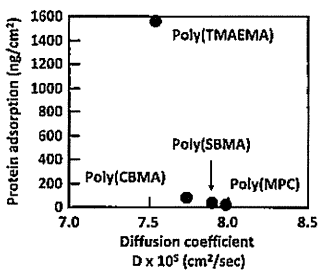

Fig. 5. Relationship between the adsorbed amount of proteins and diffusion coefficient of water molecules .

4. CONCLUSION

We researched the effect of molecular dynamics of water on protein adsorption behavior on well-defined polymer brush surface. First, we could successfully fabricate the polymer brush layers with varying chemical structures. Then, the surface-specific hydration state could be evaluated using the relaxation time measurement of water enclosed among the micro-silica beads. It is clarified that the zwitterionic polymer brush layers would be effective to reduce interaction with proteins. Interrelation between protein adsorption and hydration state at the materials surface was suggested. Control of polymer brush layer at the surface focusing on the dynamics of water molecules will realize the zero protein adsorption surfaces.

Acknowledgements

We thank to Prof. Madoka Takai, The University of Tokyo and Dr. Takehiko Tsukahara, Tokyo Institute of Technology, for their hearty and constructive discussions for this research.

References

[1] H. Chen, L. Yuan, W. Song, Z. Wu, D. Li, *Prog. Polym. Sci.* 33 (2008) 1059–1087.

[2] D. R. Lu, S. J. Lee, K. Park: *J. Biomater. Sci. Polym. Edn.* 3 (1991) 127-147

[3] K. Ishihara, H. Nomura, T. Mihara, K. Kurita, Y. Iwasaki, N. Nakabayashi, *J. Biomed. Mater. Res.* 39 (1998) 323-330.

[4] H. Kitano, K. Sudo, K. Ichikawa, M. Ide, K. Ishihara, *J. Phys. Chem.* 104 (2000) 10425-10429

[5] H. Kitano, M. Imai, T. Mori, M. Gemmei-Ide, Y. Yokoyama, K. Ishihara, *Langmuir* 19 (2003) 10260-10266.

[6] H. Kitano, S. Tada, T. Mori, K. Takaha, M. Gemmei-Ide, M. Tanaka, M. Fukuda, Y. Yokoyama, *Langmuir* 21 (2005) 11932-11940.

[7] M. Tanaka, A. Mochizuki, *J. Biomed. Mater. Res. A* 68 (2004) 684-695.

[8] S. Morita, M. Tanaka, Y. Ozaki, *Langmuir* 23 (2007) 3750-3761.

[9] T. Tsukahara, W. Misutani, K. Mawatari, T. Kitamori, *J. Phys. Chem. B* 113 (2009) 10808-10816.

[10] T. Tsukahara, A.Hibara, Y. Ikeda, T. Kitamori, *Angew. Chem.* 46 (2007) 1180-1183.

[11] K. Matyjaszewski, P. Miller, N. Shukla, B. Immaraporn, A. Gelman, B. Luokala, T. Siclovan, G. Kickelbick, T. Vallant, H. Hoffmann, T. Pakula, *Macromolecules* 32 (1999) 8716-8724.

[12] T. Ohkubo, H. Kikuchi, M. Ymaguchi, *Phys. Chem. Earth* 33 (2008) 169-176.

[13] X. Guichet, M. Fleury, E. Kohler, *J. Colloid Interface Sci.* 327 (2008) 84-93.

[14] A. Dolatshahi-Pirouz, K. Rechendorff, M. B. Hovgaard, M. Foss, J. Chevallier, F. Besenbacher, *Colloids Surf. B: Biointerfaces* 66 (2008) 53–59.

[15] A.G. Hemmersam, M. Foss, J. Chevallier, F. Besenbacher, *Colloids Surf. B: Biointerfaces* 43 (2005) 208–215.

[16] K. Ishihara, T. Ueda, N. Nakabayashi, *Polym. J.* 22 (1990) 355–360.

[17] Y. Inoue, K. Ishihara, *Colloids Surf. B: Biointerfaces* 81 (2010) 350–357.

[18] M.Kikuchi, Y.Terayama, T. Ishikawa, T. Hoshino, M. Kobayashi, H. Ogawa, H.Masunaga, J-I. Koike, M. Horigome, K. Ishihara, A. Takahara, *Polym. J.*, 44 (2012) 121-130.

[19] M. Kobayashi, H. Yamaguchi, Y. Terayama, Z. Wang, K. Ishihara, M. Hino, A. Takahara, *Macromol. Sympo.* 279 (2009) 79-87.

(Received 15 January 2012; Accepted 27 May 2012)

(Received 15 January 2012; Accepted 27 May 2012)

Biomaterials 33 (2012) 4451–4459

Contents lists available at SciVerse ScienceDirect

Biomaterials

journal homepage: www.elsevier.com/locate/biomaterials

Biomimetic hydration lubrication with various polyelectrolyte layers on cross-linked polyethylene orthopedic bearing materials

Masayuki Kyomoto [a,b,d], Toru Moro [b,c], Kenichi Saiga [a,b,d], Masami Hashimoto [e], Hideya Ito [c], Hiroshi Kawaguchi [c], Yoshio Takatori [b,c], Kazuhiko Ishihara [a,*]

[a] Department of Materials Engineering, School of Engineering, The University of Tokyo, 7-3-1 Hongo, Bunkyo-ku, Tokyo 113-8656, Japan
[b] Division of Science for Joint Reconstruction, Graduate School of Medicine, The University of Tokyo, 7-3-1 Hongo, Bunkyo-ku, Tokyo 113-8656, Japan
[c] Sensory & Motor System Medicine, Faculty of Medicine, The University of Tokyo, 7-3-1 Hongo, Bunkyo-ku, Tokyo 113-8656, Japan
[d] Research Department, Japan Medical Materials Corporation, 3-3-31 Miyahara, Yodogawa-ku, Osaka 532-0003, Japan
[e] Materials Research and Development Laboratory, Japan Fine Ceramics Center, 2-4-1 Mutsuno, Atsuta-ku, Nagoya 456-8587, Japan

ARTICLE INFO

Article history:
Received 28 December 2011
Accepted 7 March 2012
Available online 30 March 2012

Keywords:
Joint replacement
Polyethylene
Surface modification
Biomimetic material
Wear mechanism

ABSTRACT

Natural joints rely on fluid thin-film lubrication by the hydrated polyelectrolyte layer of cartilage. However, current artificial joints with polyethylene (PE) surfaces have considerably less efficient lubrication and thus much greater wear, leading to osteolysis and aseptic loosening. This is considered a common factor limiting prosthetic longevity in total hip arthroplasty (THA). However, such wear could be mitigated by surface modification to mimic the role of cartilage. Here we report the development of nanometer-scale hydrophilic layers with varying charge (nonionic, cationic, anionic, or zwitterionic) on cross-linked PE (CLPE) surfaces, which could fully mimic the hydrophilicity and lubricity of the natural joint surface. We present evidence to support two lubrication mechanisms: the primary mechanism is due to the high level of hydration in the grafted layer, where water molecules act as very efficient lubricants; and the secondary mechanism is repulsion of protein molecules and positively charged inorganic ions by the grafted polyelectrolyte layer. Thus, such nanometer-scaled hydrophilic polymers or polyelectrolyte layers on the CLPE surface of acetabular cup bearings could confer high durability to THA prosthetics.

1. Introduction

The number of artificial hip and knee joints used for primary and revised hip replacement is increasing substantially every year all over the world [1]. Most patients who receive an artificial joint experience dramatic pain relief and rapid improvement in their daily activities as well as quality of life. The most popular artificial hip joint system is a bearing couple composed of polyethylene (PE; currently cross-linked PE or CLPE) and a cobalt–chromium–molybdenum (Co–Cr–Mo) alloy. However, osteolysis has emerged as a serious issue that limits the duration and clinical outcome of artificial hip joints [2,3]. Osteolysis is triggered by a host of inflammatory responses to PE wear particles originating from the interface [4], which undergo phagocytosis by macrophages and thus induce secretion of bone resorptive cytokines [5]. Hence, different combinations of bearing surfaces and improvements in bearing materials have been studied with the aim of reducing the number of PE wear particles and extending the longevity of artificial hip joint [6–13]. However, few studies have explored methods to enhance the lubrication at the articular interface of artificial hip joints.

The bearing surfaces of a natural synovial joint are covered with a specialized type of hyaline cartilage, i.e., articular cartilage, which protects the joint interface from mechanical wear and facilitates a smooth motion of joints during daily activity [14,15]. The articular cartilage consists of chondrocytes, surrounding matrix macromolecules (e.g., proteoglycans, glycosaminoglycans, and collagens) and surface active phospholipids (SAPL; e.g., phosphatidylcholine derivatives). Due to their charge, they can trap water to maintain the water-fluid and electrolyte balance in the articular cartilages, which provides hydrophilicity and works as an effective boundary lubricant [16,17]. The fluid thin-film lubrication by the hydrated polyelectrolyte layer of articular cartilage is essential for the smooth motion of natural synovial joints. Given that learning from and mimicking nature is a widely successful theme in science and technology, it seems promising to

* Corresponding author. Tel.: +81 3 5841 7124; fax: +81 3 5841 8647.
E-mail address: ishihara@mpc.t.u-tokyo.ac.jp (K. Ishihara).

0142-9612/$ – see front matter © 2012 Elsevier Ltd. All rights reserved.
doi:10.1016/j.biomaterials.2012.03.028

investigate surface modification of bearing surfaces in artificial joints to mimic the role of cartilage.

Grafting of polymeric molecules onto a substrate through covalent bonding is a well-known method for modifying a polymer surface [18]. Grafting polymerization is mostly performed using either of the following methods: (1) surface-initiated graft polymerization, termed the "grafting from" method, in which monomers are polymerized from initiators or comonomers; and (2) adsorption of the polymer to the substrate, termed the "grafting to" method (i.e., dipping, cross-linking, and ready-made polymers reacting with the substrate) [19,20]. The former method has an advantage over the latter method in that it synthesizes a semi-dilute or high-density polymer brush [21].

In this study, we synthesized nanometer-scale hydrophilic layers on the CLPE surface of an artificial hip joint to reduce wear and avoid bone resorption. Our strategy is to modify the bearing surfaces of artificial joints with a hydrophilic polyelectrolyte layer to increase lubrication to levels that match articular cartilage under physiological conditions. Such nanometer-scale surface modification was accomplished using a photoinduced radical polymerization technique similar to the "grafting from" method; this approach renders only the surface of the CLPE substrate susceptible to modification and does not affect the bulk properties [22,23]. In addition, we investigated the effect of polyelectrolyte layers with various lubrication conditions on hydration lubrication [24] to realize the hydrophilicity and lubricity of the physiological joint surface. Such investigations are of great importance in the design of lubricated surfaces for artificial joints, and in better understanding the lubrication mechanisms of both natural and artificial joints. Here, we asked whether (1) the hydrophilic polymer or polyelectrolyte characteristics (i.e., nonionic, cationic, anionic, or zwitterionic) would affect the hydration- and friction-kinetics of the hydration layer and (2) the hydration lubrication characteristics of the polyelectrolyte layers might assure the durability of artificial hips.

2. Materials and methods

2.1. Chemicals

Benzophenone and acetone were purchased from Wako Pure Chemical Industries, Ltd. (Osaka, Japan). Oligo(ethylene glycol) methacrylate (M_n = 360; OEGMA) and 2-(dimethylamino)ethyl methacrylate (DMAEMA) were purchased from Sigma–Aldrich Corp. (Saint Louis, MO, USA) and Tokyo Chemical Industry Co., Ltd. (Tokyo, Japan), respectively (Fig. 1A). 2-Methacryloyloxyethyl phosphate (MPA) was extracted from an aqueous suspension of Phosmer M solution (Unichemical Co., Ltd., Ikoma, Japan) with *n*-hexane (Kanto Chemical Co., Inc., Tokyo, Japan). 2-Methacryloyloxyethyl phosphorylcholine (MPC) was industrially synthesized by using the method reported by Ishihara et al. and supplied by NOF Corp. (Tokyo, Japan) [25].

2.2. Graft polymerization with various polyelectrolytes

A compression-molded PE (GUR1020 resin; Quadrant PHS Deutschland GmbH, Vreden, Germany) sheet stock was irradiated with a 50-kGy dose of gamma-rays in N_2 gas and annealed at 120 °C for 7.5 h in N_2 gas in order to facilitate cross-linking. CLPE specimens were then machined from this sheet stock after cooling.

These CLPE specimens were immersed in an acetone solution containing 10 mg/mL benzophenone for 30 s and then dried at room temperature in order to remove the acetone. Each monomer was dissolved in degassed pure water to obtain a 0.50-mol/L monomer aqueous solution, and the CLPE specimens coated with benzophenone were immersed in this solution. Photoinduced graft polymerization on the CLPE surface was performed using UV irradiation (UVL-400HA ultra-high pressure mercury lamp; Riko-Kagaku Sangyo Co., Ltd., Funabashi, Japan) with an intensity of 5 mW/cm^2 at 20 °C (DMAEMA) [26] or 60 °C (OEGMA, MPA, MPC) for 23–180 min (Fig. 1B); a filter (Model D-35; Toshiba Corp., Tokyo, Japan) was used to restrict the UV light to wavelengths of 350 ± 50 nm [27,28]. After polymerization, each of the poly(OEGMA) (POEGMA)-, poly(DMAEMA) (PDMAEMA)-, poly(MPA) (PMPA)-, and poly(MPC) (PMPC)-grafted CLPE specimens was removed, washed with pure water and ethanol, and dried at room temperature. These and untreated CLPE (as control) specimens were sterilized by with a 25-kGy dose of gamma-rays under N_2 gas [29].

2.3. Cross-sectional observation by transmission electron microscopy

A cross-section of the various polyelectrolyte-grafted layers on the CLPE surface with a 90-min photoirradiation time was observed under a transmission electron microscope (TEM). The specimens were embedded in epoxy resin, stained with ruthenium oxide vapor at room temperature, and finally sliced into ultra-thin films (approximately 100-nm-thick) by using a Leica Ultra Cut UC microtome (Leica Microsystems, Ltd., Wetzlar, Germany). The specimens of the various polyelectrolyte-grafted CLPE were pre-coated with a platinum–palladium thin film before embedding in epoxy resin to preserve the graft layer. A JEM-1010 electron microscope (JEOL, Ltd., Tokyo, Japan) was used for the TEM observations at an acceleration voltage of 100 kV.

2.4. Surface analysis of various polyelectrolyte-grafted CLPEs

The functional group vibrations of the various polyelectrolyte-grafted CLPE surfaces with a 90-min photoirradiation time were examined by Fourier-transform infrared (FT-IR) spectroscopy with attenuated total reflection (ATR) equipment. The FT-IR/ATR spectra were obtained using an FT-IR analyzer (FT/IR615; JASCO Co. Ltd., Tokyo, Japan) for 32 scans over the range 800–2000 cm^{-1} at a resolution of 4.0 cm^{-1}.

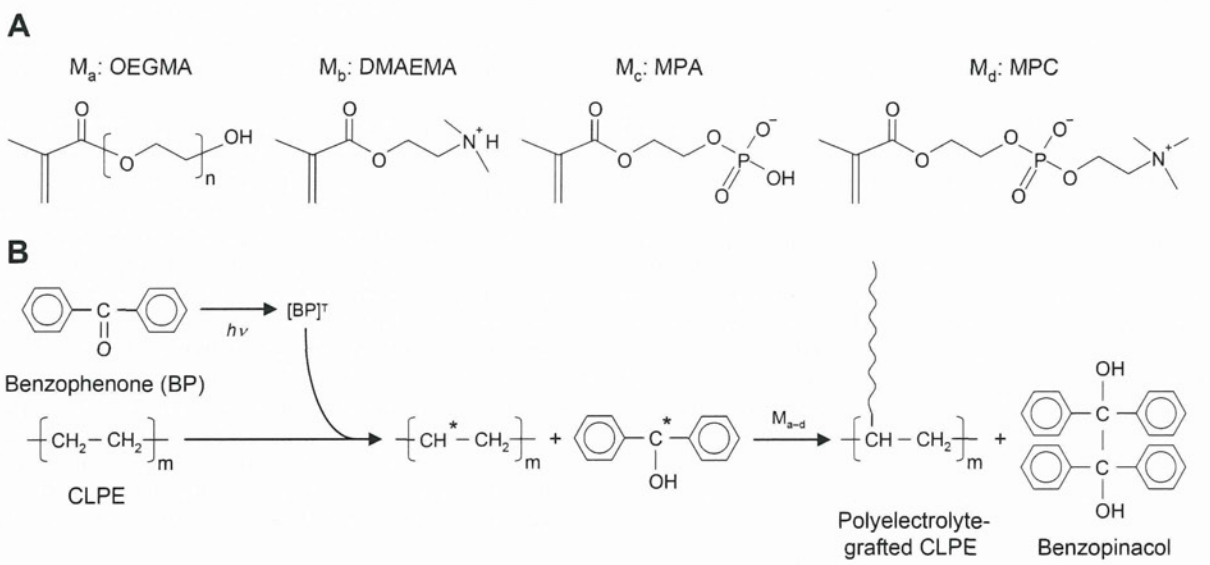

Fig. 1. Schematic illustration showing the preparation of various polyelectrolyte-grafted CLPE. (A) Monomers and (B) photoinduced graft polymerization.

The surface elemental conditions of the various polyelectrolyte-grafted CLPE surfaces with a 90-min photoirradiation time were analyzed by X-ray photoelectron spectroscopy (XPS). The XPS spectra were obtained using an XPS spectrophotometer (AXIS-HSi165; Kratos/Shimadzu Co., Kyoto, Japan) equipped with a 15-kV Mg-Kα radiation source at the anode. The take-off angle of the photoelectrons was maintained at 90°. Five scans were taken for each sample.

The static-water contact angles on the various polyelectrolyte-grafted CLPE surfaces obtained at various photoirradiation times were measured by the sessile drop method using an optical bench-type contact angle goniometer (Model DM300; Kyowa Interface Science Co., Ltd., Saitama, Japan). Drops of purified water (1 μL) were deposited on the various polyelectrolyte-grafted CLPE surfaces, and the contact angles were directly measured with a microscope 60 s after dropping. Measurements were repeated 15 times for each sample, and the average values were regarded as the contact angles.

2.5. Friction test

Friction tests were performed using a ball-on-plate machine (Tribostation 32; Shinto Scientific Co., Ltd., Tokyo, Japan) with various lubrication conditions. Each of the various polyelectrolyte-grafted CLPE surfaces was used to prepare six sample pieces. A 9-mm-diameter ball of Co–Cr–Mo alloy was prepared. The surface roughness (R_a) of the pin was less than 0.01 μm, which is comparable to that of femoral head products. The friction tests were performed with a load of 0.98 N (contact stress roughly calculated by Hertzian theory is approximately 29 MPa), sliding distance of 25 mm, and a frequency of 1 Hz for a maximum of 100 cycles. The lubricants used were pure water at room temperature, acellular simulated body fluid (SBF, Kokubo solution, pH 7.4) with inorganic ion concentrations analogous to those found in human extracellular fluid at 37 °C [30], and a mixture of 25-vol% bovine serum at 37 °C. Before the friction tests, the specimens were pre-soaked in each lubricant for 24 h. The coefficient of dynamic friction for each specimen was determined by averaging five data points from the 100 (96–100) cycle measurements, and the average values for six sample pieces are reported as the mean coefficient of dynamic friction for each of the various polyelectrolyte-grafted CLPE surfaces.

2.6. Surface zeta potential measurement

The effective surface charge of the various polyelectrolyte-grafted CLPE surfaces was determined via an electrophoretic mobility method with an electrophoretic light-scattering spectrophotometer (ELS-800; Otsuka Electronics Co., Ltd., Osaka, Japan) equipped with a solid-plate sample cell. Before measurement, the specimens were equilibrated by soaking in a 0.01-mol/L sodium chloride aqueous solution for 1 h. The measurement was carried out in a 0.01-mol/L sodium chloride aqueous solution at 20 °C. Six samples for each of the various polyelectrolyte-grafted CLPE surfaces were prepared for the measurements, and the average values are reported as the surface zeta potential.

2.7. Characterization of protein adsorption by micro bicinchoninic acid method

The amount of protein adsorbed on the various polyelectrolyte-grafted CLPE surfaces was measured by the micro bicinchoninic acid (BCA) method. For each type of polyelectrolyte-grafted CLPE, ten sample pieces were prepared. Each specimen was immersed in Dulbecco's phosphate buffered saline (PBS; pH 7.4; ionic strength, 0.15 M; Immuno-Biological Laboratories Co., Ltd., Takasaki, Japan) for 1 h to equilibrate the polymer-grafted surface. The specimens were then immersed in bovine serum albumin (BSA; $M_w = 6.7 \times 10^4$; Sigma–Aldrich Corp., MO, USA) solution at 37 °C for 1 h. The protein solution was prepared at a BSA concentration of 4.5 g/L, i.e., 10% of the concentration of human plasma levels. Then, the specimens were rinsed five times with fresh PBS, immersed in a 1-mass% sodium dodecyl sulfate (SDS) aqueous solution, and shaken at room temperature for 1 h to detach completely the adsorbed BSA from the polymer-grafted CLPE surface. A protein analysis kit (micro BCA protein assay kit, #23235; Thermo Fisher Scientific Inc., IL, USA) based on the BCA method was used to determine the BSA concentration in the SDS solution, and this value was used to determine the amount of BSA adsorbed on the polyelectrolyte-grafted CLPE surface.

2.8. Hip simulator wear test

A 12-station hip simulator (MTS Systems Corp., Eden Prairie, MN) with untreated CLPE and the various polyelectrolyte-grafted CLPE cups, each with inner and outer diameters of 26 and 52 mm, respectively, was used for the wear test according to the ISO standard 14242-3. Three sample pieces were prepared for each untreated CLPE and the various polyelectrolyte-grafted CLPE cups. A Co–Cr–Mo alloy ball with a diameter of 26 mm (K-MAX® HH-02; Japan Medical Materials Corp., Osaka, Japan) was used as the femoral component. A mixture of 25-vol% bovine serum was used as the lubricant, which was replaced every 0.5×10^6 cycles. Gait cycles were applied that simulated a physiological loading curve (Paul-type) with double peaks at 1793 and 2744 N (maximum contact stress roughly calculated by Hertzian theory is approximately 8 MPa) with a multidirectional (biaxial and orbital) motion at 1-Hz frequency. Gravimetric wear was determined by weighing the cups at intervals of 0.5×10^6 cycles. Load-soak controls ($n = 2$) were used to compensate for the fluid absorption by the specimens according to the ISO standard 14242-2. Testing was continued until a total of 3.0×10^6 cycles was completed. When the gravimetric method was used, the weight loss of the tested cups was corrected by subtracting the weight gain in the load-soak controls; however, this correction was not perfect because only the tested cups were continuously subjected to the motion and the load. In addition, after 3.0×10^6 cycles of the hip simulator test, the volumetric wear of the cups was measured using a three-dimensional coordinate measurement machine (BHN-305; Mitsutoyo Corp., Kawasaki, Japan) and reconstructed using three-dimensional modeling software (Imageware; Siemens PLM Software Inc., Plano, TX).

Wear particles were observed under a field emission scanning electron microscope (FE-SEM). The wear particles were isolated from the bovine serum solution used as lubricant in the hip simulator wear tests. To isolate the wear particles, the lubricant was incubated in a 5-mol/L sodium hydroxide solution for 3 h at 65 °C to digest adhesive proteins that were degraded and precipitated. To avoid artifacts, the contaminating proteins were removed by extraction with solutions having several densities: sugar solution, 1.20 g/cm^3 and 1.05 g/cm^3; and isopropyl alcohol solution, 0.98 g/cm^3 and 0.90 g/cm^3. This was followed by centrifugation at 25,500 rpm for 3 h at 5 °C (himac CP 70MX; Hitachi Koki Co., Ltd, Tokyo, Japan). The collected solution was sequentially filtered through a 0.1-μm membrane filter, and the membrane was observed directly under an FE-SEM (JSM-633OF; JEOL DATUM Co., Ltd, Tokyo, Japan) at an acceleration voltage of 20 kV after gold deposition.

2.9. Statistical analysis

The mean values of the groups (untreated and various polyelectrolyte-grafted CLPE) were compared by one-factor analysis of variance (ANOVA) and the significance of differences in the static-water contact angle (static-water contact angle measurement), dynamic friction coefficient (ball-on-plate friction test), surface zeta potential (surface zeta potential measurement), and amount of adsorbed BSA (protein adsorption measurement by micro BCA method) were determined by post-hoc testing using Bonferroni's method. The statistical significance of gravimetric wear (hip simulator test) was judged by the Student's *t*-test. All statistical analyses were performed using add-on software (Statcel 2; OMS publishing Inc., Tokorozawa, Japan) for a computerized worksheet (Microsoft Excel® 2003; Microsoft Corp., Redmond, WA).

3. Results

As shown in the cross-sectional TEM images in Fig. 2, all graft polymerization processes afforded a uniform grafted polyelectrolyte layer on the CLPE surface with almost constant thicknesses of 100–150 nm.

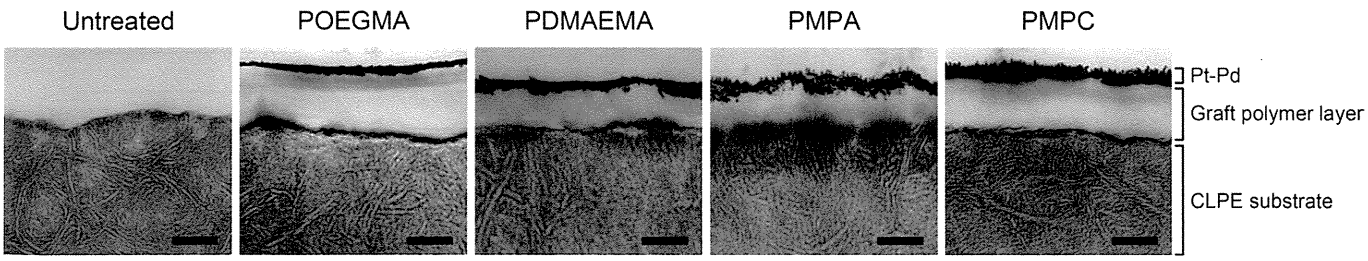

Fig. 2. Cross-sectional TEM images of untreated CLPE and various polyelectrolyte-grafted CLPE samples obtained with a 90-min photoirradiation time. Bar: 100 nm.

Fig. 3 shows the FT-IR/ATR and XPS spectra of the untreated CLPE and various polyelectrolyte-grafted CLPE samples subjected to photoirradiation for a 90 min. The FT-IR/ATR spectra after grafting contained new absorption peaks at 1720 cm^{-1} (C=O); 1090 and 1040 cm^{-1} (ether or carbohydrate group); 1140 and 960 cm^{-1} (protonated or carbonated ammonium group); and 1240, 1080, and 970 cm^{-1} (phosphate group) for each of the polyelectrolyte-grafted CLPE samples. These peaks are chiefly attributed to the graft polymer on each CLPE surface. The XPS spectra of the binding energy region of the nitrogen (N) and/or phosphorous (P) electrons showed peaks for the PDMAEMA-, PMPA-, and PMPC-grafted CLPE samples, whereas peaks were not observed for untreated CLPE and the POEGMA-grafted CLPE samples. The peaks at 400 and 403 eV are attributed to N–H, $-NH^{+}(CH_3)_2$, and $-N^{+}(CH_3)_3$, respectively. The peak at 134 eV is attributed to the phosphate groups. These peaks indicate the presence of a dimethylamino group in the DMAEMA units, phosphonooxy group in the MPA units, and phosphorylcholine group in the MPC units. Overall, these results from TEM observation, FT-IR/ATR, and XPS analyses indicate that the various polyelectrolytes were successfully grafted on the CLPE surface.

Next, as shown in Fig. 4, the static-water contact angle was 95° for untreated CLPE and this value decreased as the photoirradiation time increased. Thus, clearly, the photoirradiation time affected the hydration-kinetics of the polyelectrolyte graft chains. However, the decrease (or decrease rate) of the static-water contact angle differed for each of the polyelectrolyte-grafted CLPE surfaces. Nevertheless, after photoirradiation for more than 90 min (45 min for POEGMA-grafted CLPE), the static-water contact angles of all polyelectrolyte-grafted CLPE samples reached the lowest values of 20°–60°.

Fig. 5 shows the coefficient of dynamic friction of polyelectrolyte-grafted CLPE samples obtained with a 90-min photoirradiation time in various lubricants. Control measurements were carried out in water as the lubricant. From the figure, we see that the coefficients of dynamic friction for the polyelectrolyte-grafted CLPE samples were 0.01–0.05, representing a 40%–85% reduction compared with untreated CLPE. A calcification-like mineralized surface morphology was observed on the PMPA-grafted CLPE surface after SBF pre-soaking for 24 h before the friction test. The coefficient of dynamic friction of the POEGMA- and PMPC-grafted CLPE surfaces did not differ significantly ($p > 0.05$) between lubricants. The coefficient of dynamic friction of PMPC-grafted CLPE was significantly ($p < 0.01$) lower than that of POEGMA-grafted CLPE under each lubrication condition; the same relation was found for the static-water contact angles of the two types of polyelectrolyte-grafted CLPE surfaces. In contrast, the coefficient of dynamic friction of the PDMAEMA- and PMPA-grafted CLPE surfaces increased drastically ($p < 0.01$) in SBF and BS, respectively. In addition, the untreated CLPE also showed increased friction in BS lubricant compared with that in water.

Fig. 6 shows the surface zeta potential and the amount of BSA adsorbed on the untreated CLPE and the various polyelectrolyte-grafted CLPE samples with a 90-min photoirradiation time. As seen in the figure, the surface zeta potential of the untreated CLPE and the POEGMA- and PMPC-grafted CLPE surfaces with nonionic and zwitterionic grafted polymer layers was close to zero (Fig. 6A). In contrast, that of PDMAEMA-grafted CLPE with cationic grafted polymer layers was 50.6 mV, which is strongly positive, and that of PMPA-grafted CLPE with anionic grafted polymer layers was −32.5 mV, which is strongly negative. The amount of adsorbed BSA on the POEGMA-, PMPA-, and PMPC-grafted CLPE surfaces with nonionic, anionic, and zwitterionic grafted polymer layers significantly ($p < 0.01$) decreased (Fig. 6B). In contrast, that of PDMAEMA-grafted CLPE with a cationic grafted polymer layer increased ($p < 0.01$).

Fig. 7 shows how the polyelectrolyte hydrated layer characteristics affected the durability of artificial hips. Three-dimensional

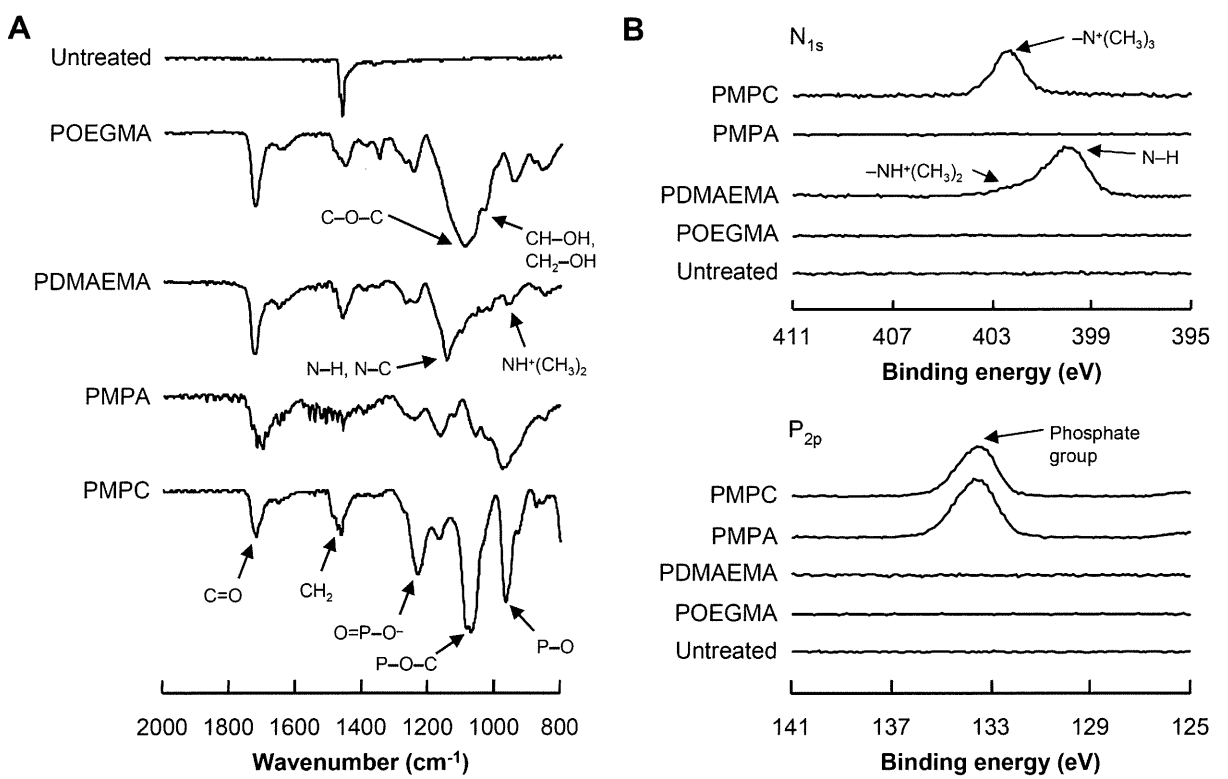

Fig. 3. (A) FT-IR/ATR and (B) XPS spectra of untreated CLPE and various polyelectrolyte-grafted CLPE samples obtained with a 90-min photoirradiation time.

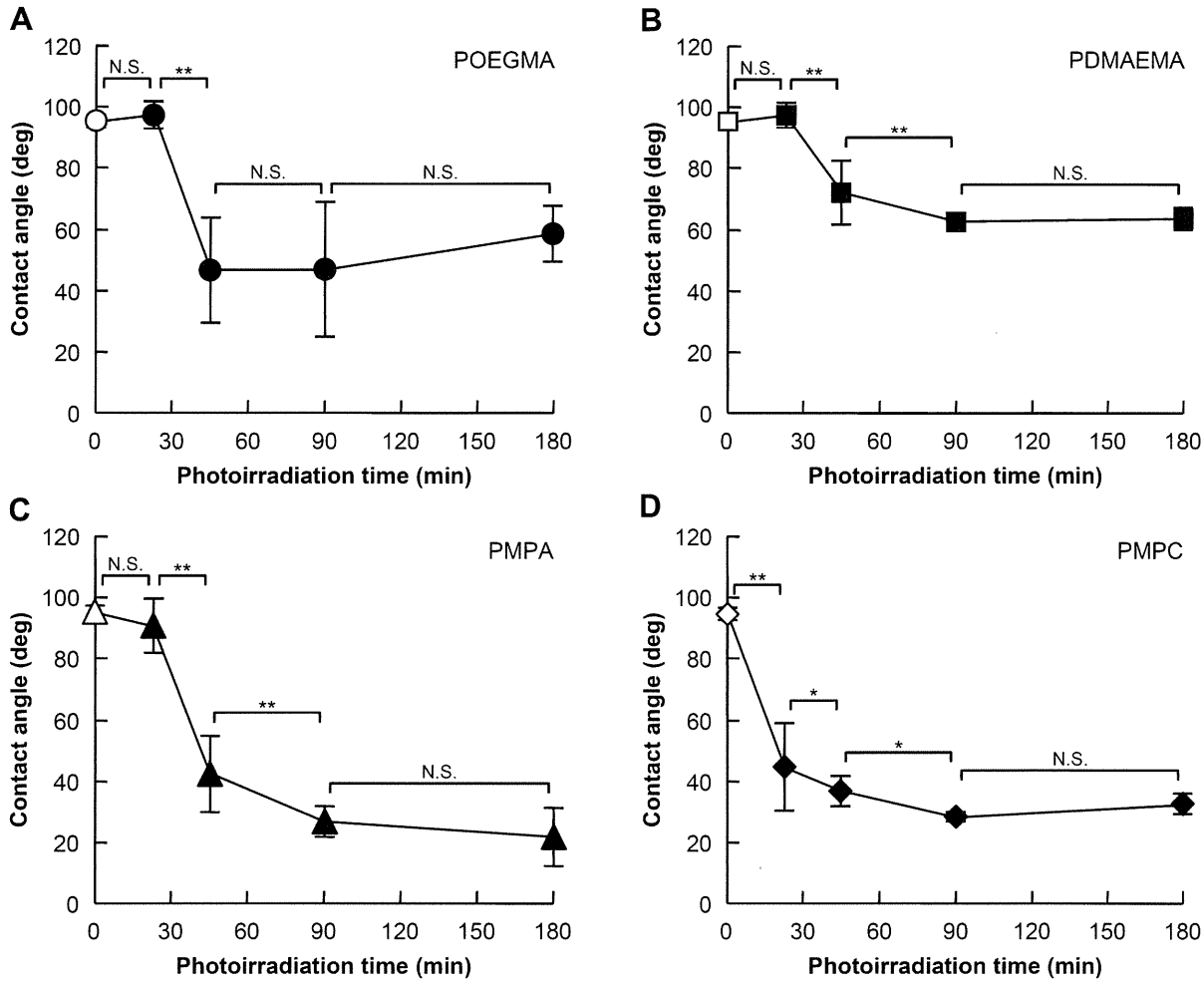

Fig. 4. Static-water contact angle on various polyelectrolyte-grafted CLPE surfaces as a function of the photoirradiation time. (A) POEGMA-grafted, (B) PDMAEMA-grafted, (C) PMPA-grafted, and (D) PMPC-grafted CLPE. Data are expressed as means ± standard deviations. * Indicates $p < 0.05$, ** indicates $p < 0.01$, and N.S. indicates no statistical difference.

coordinate measurements with the polyelectrolyte-grafted CLPE cups revealed little to no detectable volumetric wear, although substantial volumetric wear was detected in the untreated CLPE (Fig. 7A). The wear particles of untreated CLPE and polyelectrolyte-grafted CLPE cups after 0.5–1.0 × 10^6 cycles of the hip simulator test, as characterized by FE-SEM, were predominantly sub-micrometer-sized granules (Fig. 7B). In all cases, the morphologies of the wear particles exhibited no remarkable difference. However, remarkably fewer wear particles were found for POEGMA- and PMPC-grafted CLPE cups than for untreated CLPE cups.

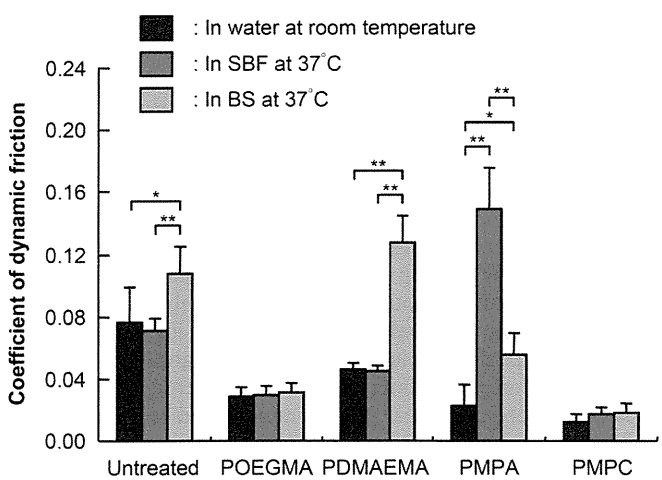

Fig. 5. Coefficient of dynamic friction of polyelectrolyte-grafted CLPE samples obtained with a 90-min photoirradiation time in the ball-on-plate friction test under various lubrication conditions. Data are expressed as means ± standard deviations. * Indicates $p < 0.05$, ** indicates $p < 0.01$, and N.S. indicates no statistical difference.

Fig. 8 shows the time course of gravimetric wear of the various polyelectrolyte-grafted CLPE cups during the hip simulator test. PDMAEMA-, POEGMA-, and PMPC-grafted CLPE cups were found to undergo significantly less gravimetric wear than untreated CLPE cups. These gravimetric wear results support the volumetric wear images in Fig. 7A. Furthermore, POEGMA- and PMPC-grafted CLPE cups showed a slight, gradual increase in weight during the hip simulator test. This is partially attributable to greater fluid (e.g., water, proteins, and lipids) absorption in the tested cups than in the load-soak controls. Note that when using the gravimetric method, the weight loss of the tested cups was corrected by subtracting the weight gain in the load-soak controls; however, this correction is not perfect because only the tested cups are continuously subjected to motion and load.

4. Discussion

In natural synovial joints under physiological conditions, fluid film lubrication by the hydrated layer is essential for the smooth

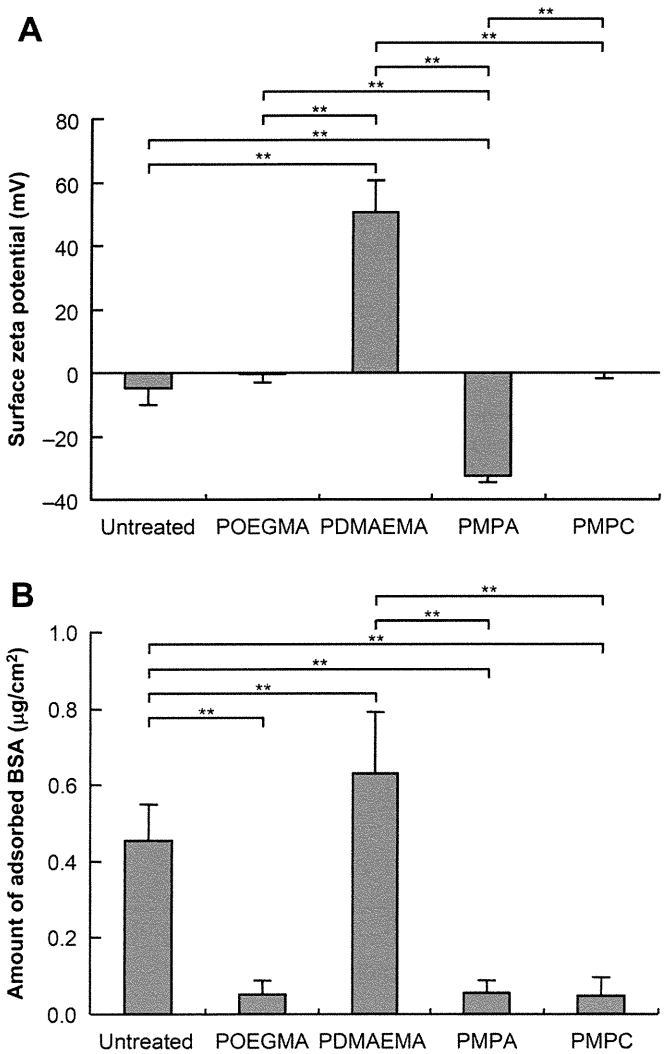

Fig. 6. Surface zeta potential and the amount of adsorbed BSA for untreated CLPE and the various polyelectrolyte-grafted CLPE samples with a 90-min photoirradiation time. Data are expressed as means ± standard deviations. ** Indicates $p < 0.01$.

motion of joints [31], and a nanometer-scaled hydrated polyelectrolyte layer that covers the joint cartilage surface provides hydrophilicity and works as an effective boundary lubricant [14–17]. Hence, grafting a cartilage-like hydrophilic polymer layer onto the bearing surface of an artificial joint may afford the same hydrophilicity and lubricity of the physiological joint surface [32]. With this viewpoint, we specifically investigated whether (1) the hydrophilic polymer or polyelectrolyte characteristics would affect the hydration- and friction-kinetics of the hydration layer and (2) the characteristics of hydration lubrication [24] of polyelectrolyte layers might assure the durability of artificial hips.

The results of the TEM, FT-IR/ATR, and XPS analyses confirmed successful synthesis of nanometer-scale hydrophilic layers with varying charge (nonionic/neutral, cationic, anionic, or zwitterionic properties) on a CLPE surface. The results also showed that the hydrophilicity of each of the various polyelectrolyte-grafted CLPE surfaces gradually increased with the photoirradiation time, as previously reported (Fig. 4) [23]. To obtain a uniform graft layer on a CLPE surface, the photoirradiation time during graft polymerization must be controlled [27]. Controlled 100-nm-thick, uniform graft layers with varying charge are essential for a proper comparison of friction and wear performance under various lubricant conditions.

Specifically, the results of the present study show that the charge (nonionic, cationic, anionic, or zwitterionic) of the graft layer affects the hydration- and friction-kinetics of the CLPE bearing surface; the coefficient of dynamic friction in ball-on-plate friction test with a water lubricant depends on the hydrophilicity (static-water contact angles) as shown in Figs. 4 and 5. All of the polyelectrolyte-grafted CLPE surfaces exhibited considerably higher lubricity than the untreated CLPE surface in a water lubricant. This is because the water molecules in the hydration layers of the hydrophilic polymer or polyelectrolytes act as very efficient lubricants [32,33]. However, in other lubricant conditions, the polyelectrolyte-grafted CLPE surfaces with cationic and anionic polymer layer exhibited significantly different characteristics compared with neutral hydrophilic polymer- or zwitterionic polyelectrolyte-grafted CLPE surfaces, even though all showed high hydrophilicity.

The PDMAEMA-grafted CLPE samples exhibited a higher coefficient of dynamic friction in the BS lubricant containing proteins (e.g., albumin, globulin) than in water or SBF lubricants in the ball-on-plate friction test [34]. PDMAEMA has a positively charged $-NH^{+}(CH_3)_2$ group at neutral pH, which in turn attracts negatively charged molecules (e.g., albumin molecules have negatively charges at neutral pH) (Fig. 6). This implies that the existence of protein molecules at the bearing interface increases the resistance to sliding motion. Since protein is adsorbed on the Co–Cr–Mo alloy counterface [35,36], the high resistance to sliding motion is interpreted as being the result of higher adhesive interaction or interpenetration of the adsorbed protein films formed on both PDMAEMA-grafted CLPE and Co–Cr–Mo alloy surfaces. However, the PDMAEMA-grafted CLPE cups exhibited high wear resistance in the hip simulator test at high load, despite the high coefficient of dynamic friction in the ball-on-plate friction test in the BS lubricant. This may be because the adsorbed protein film from the BS lubricant is squeezed out of the bearing interface at high load [37].

In contrast, the PMPA-grafted CLPE surfaces exhibited considerably poor lubricity in the ball-on-plate friction test with an SBF lubricant. The chemical structure of the negatively charged PMPA is characterized by the presence of a large number of trap sites for positively charged inorganic ions. Hence, the poor lubricity of PMPA-grafted CLPE surfaces is interpreted as being due to shrinkage or bridging of negatively charged polyelectrolyte chains, which reduced the mobility of the chains in a solution containing positively charged inorganic ions [32–34]. In a previous study, Kato et al. reported that PMPA-grafted poly(ethylene terephthalate) surfaces induced hydroxyl apatite deposition in SBF, mimicking biological mineralization [38]. In this study, a similar phenomenon was observed as the PMPA-grafted CLPE surfaces exhibited calcification-like mineralization after pre-soaking in SBF for 24 h before the friction test. (The chemical composition of the mineralized thin layer on the PMPA-grafted CLPE surfaces could not be detected by thin film X-ray diffraction analysis.) The BS lubricant in this hip simulator test contained not only protein molecules but also inorganic ions. Further, during the 3.0×10^6 cycles of the hip simulator test, the test cups were soaked in the BS lubricant for over 30 days. It is therefore thought that the negatively charged PMPA in turn attracts only positively charged inorganic ions and repels the negatively charged molecules; the PMPA-grafted CLPE cups exhibited higher wear than the other polyelectrolyte-grafted CLPE cups due to abrasive wear by the mineralized hardened surface layer [39].

The POEGMA- and PMPC-grafted CLPE cups exhibited high wear resistance in the hip simulator tests (Figs. 7 and 8) as well as low coefficients of dynamic friction in the ball-on-plate friction tests (Fig. 5). In particular, the highly hydrated surface layer of PMPC-grafted CLPE provided extremely efficient lubrication under all

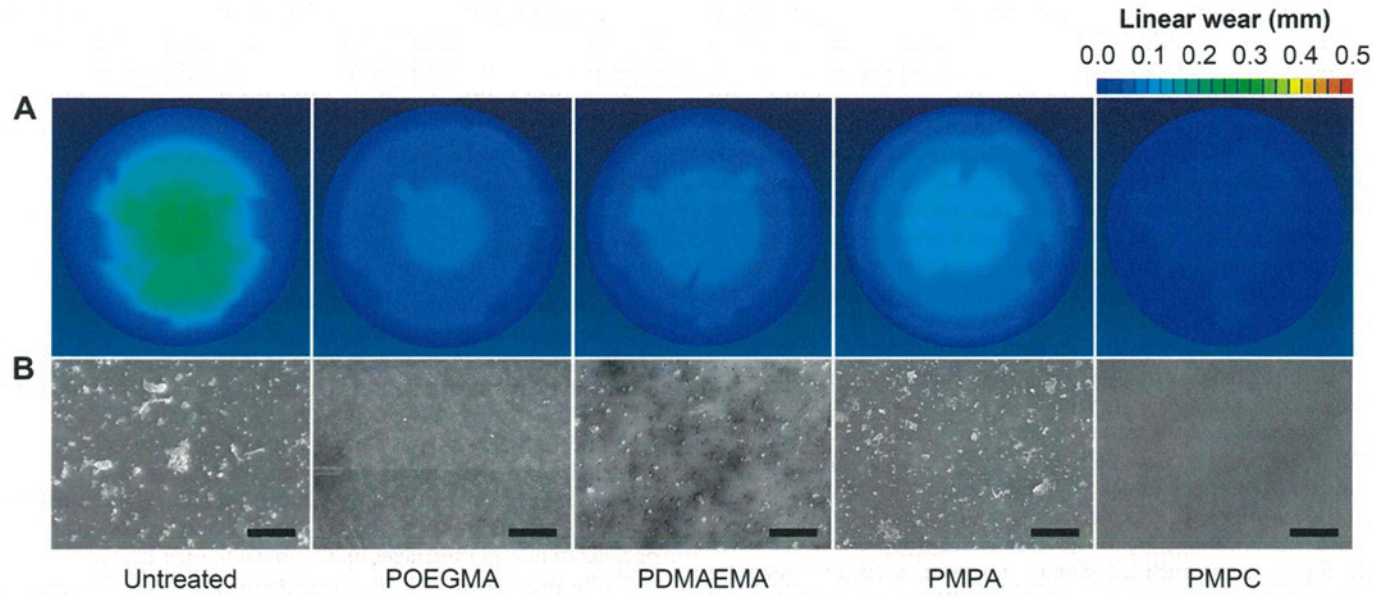

Fig. 7. Analysis of various polyelectrolyte-grafted CLPE cups after the hip simulator test. (A) Three-dimensional coordinate measurements of various polyelectrolyte-grafted CLPE cups and (B) SEM images of wear particles isolated from lubricants of the hip simulator test. Scale bar indicates 5 μm.

conditions. Moreover, the zeta potential of the PMPC-grafted CLPE surface was close to zero because the ionic group in the MPC unit forms an inner salt and the electrostatic effects are diminished. Therefore, the zwitterionic grafted polymer layers attract water molecules only, and repel the protein molecules (Fig. 6B) and positively charged inorganic ions. This characteristic is the same as that of the nonionic grafted polymer layers. Chen et al. reported that the water molecules adsorbed on the surface of highly hydrophilic polyzwitterionic (i.e., PMPC) brushes act as lubricants to reduce the interaction between the brushes and the counter-surface [40]. Recent efforts to identify hydrophilic polymers or polyelectrolytes have focused on nanotribological studies of surface-attached molecules, seeking to emulate those at the cartilage surface [32,41,42]. However, the above results for PDMAEMA- and PMPA-grafted CLPE in the hip joint simulator tests demonstrate that the mechanism of action of the polyelectrolyte-grafted layer cannot be explained simply in terms of fluid film lubrication. Therefore, we believe that the primary mechanism underlying the low friction and high wear resistance is the high level of hydration of the polyelectrolyte layer, such as the zwitterionic PMPC-grafted layer; water molecules in the hydration layers act as very efficient lubricants [32,42,43]. The secondary mechanism is attributed to a repulsion of protein molecules by the positively charged inorganic ions of the polyelectrolyte layer in a synovial fluid, which may reduce the adhesive interaction or interpenetration between opposing Co–Cr–Mo alloy surfaces or adsorbed protein films on the Co–Cr–Mo alloy [8,40].

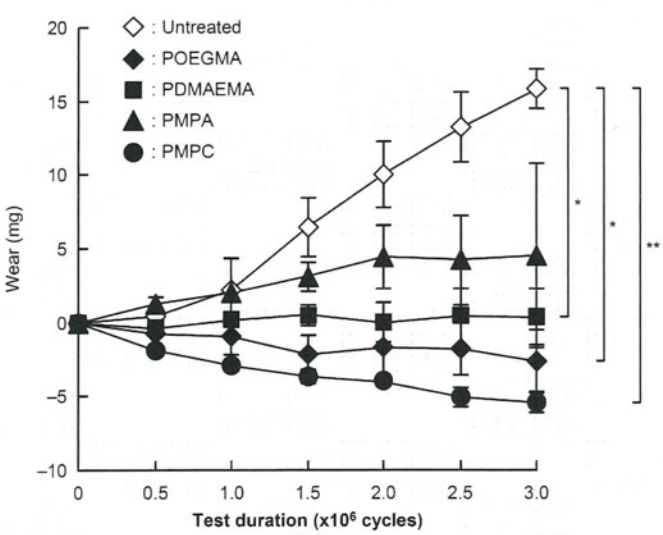

Fig. 8. Time course of gravimetric wear of various polyelectrolyte-grafted CLPE cups during the hip simulator test. Data are expressed as means ± standard deviations. * Indicates $p < 0.05$, ** indicates $p < 0.01$ as compared with an untreated CLPE cup.

After 3.0×10^6 cycles of the hip simulator test, the POEGMA-, PDMAEMA-, and PMPC-grafted CLPE cups show a greater than 97% reduction in steady wear rate (−1.82–0.12 mg/10^6 cycles) compared with untreated CLPE (Fig. 8). This suggests the approach may be promising for extending the longevity of THA prosthetics [44]. To explain this we assume that the hydrated bearing surface of the artificial joint modified with PMPC exhibited fluid film lubrication (i.e., hydration lubrication [24,45]) and suggest this artificial hip mimics the cartilage or SAPL layer on the cartilage in natural joints [23]. Although the PMPC layer has no direct analog to the cartilage surface containing SAPL, the results of the present study underline the possible importance at such surfaces of highly hydrated macromolecules in the chondroprotective and lubrication roles.

The POEGMA- and PMPC-grafted CLPE cups did not lose weight during the hip simulator test; instead, they gained weight even after correction for water absorption in the load-soak control, suggesting an underestimation of the load-soak control, as previously reported [12,46]. The cups showed comparable weight gains after 3.0×10^6 cycles, irrespective of the presence or absence of the POEGMA- and PMPC-graft layers, confirming that the weight gain was the result of the water absorbed by the cup material (i.e., the CLPE substrate) and not the result of retention of extraneous materials on the surface POEGMA- and PMPC-graft layers. These cups decreased the amount of wear particles isolated from the lubricants. Because wear particles from POEGMA- and PMPC-graft CLPE surfaces were hardly observed as a result of their extremely